

**INSIGHTS IN FUNDAMENTAL SCRATCH BEHAVIOR OF  
POLYMERIC MATERIALS**

A Thesis

by

EHSAN MOGHBELLI

Submitted to the Office of Graduate Studies of  
Texas A&M University  
in partial fulfillment of the requirements for the degree of  
MASTER OF SCIENCE

August 2007

Major Subject: Mechanical Engineering

**INSIGHTS IN FUNDAMENTAL SCRATCH BEHAVIOR OF  
POLYMERIC MATERIALS**

A Thesis

by

EHSAN MOGHBELLI

Submitted to the Office of Graduate Studies of  
Texas A&M University  
in partial fulfillment of the requirements for the degree of

MASTER OF SCIENCE

Approved by:

Chair of Committee,  
Committee Members,

Head of Department,

Hung.-Jue Sue  
Anastasia Muliana  
John Whitcomb  
Dennis O'Neal

August 2007

Major Subject: Mechanical Engineering

## **ABSTRACT**

Insights in Fundamental Scratch Behavior of Polymeric Materials.

(August 2007)

Ehsan Moghbelli, B.S., Tehran Polytechnic Institute (Amir Kabir University), Iran

Chair of Advisory Committee: Dr. Hung-Jue Sue

This work is mainly focused upon the analytical examination of the physical and mechanical response of plastics undergoing an induced scratch deformation caused by a semi-spherical scratch tip under a linearly increasing normal load. Evaluation of the scratch deformations in this study was based upon visual and optical observations and upon observations of failure and fracture mechanisms as well as Electron Microscopy examinations. In the first section of this study an effort was made to correlate the scratch resistance observed in Polypropylene (PP) thin sheets with material properties, such as molecular weight and surface crystallinity. In the second section of this work the scratch behavior of epoxy nanocomposites was examined and a conclusion was made based upon the effects of the addition of nano-additives with various natures into the epoxy matrix. Furthermore, a region of the scratch path prior to the onset of scratch visibility known as the mar region, which was an obscure area of deformation on a microscopic scale, was thoroughly investigated for the epoxy systems and various conclusions were made based upon those results.

Finally, based on these findings and previous studies, it was shown that failure

and fracture mechanisms of polymeric materials under scratch deformations are dependent on the type and physical nature of the material, whereas brittle and ductile materials show various behaviors under the specified conditions. Based on the failure mechanism which the material exhibits subsequent to the scratch deformation process and the physical and mechanical characteristics of the material, several factors were shown to effect the materials ability to scratch resistance.

## DEDICATION

*I dedicate this work to the following individuals who have all influenced my life:*

*My parents (Dr. Hassan Moghbelli and Dr. Zohreh Eslami) and brother (Dr. Meisam Moghbelli) who have been supporting my dream and giving me the reasons to be strong and keep moving on.*

*Prof. H.-J. Sue who has been providing valuable guidance for me to grow as a person and as a researcher.*

*Dr. Naser Mohammadi whose academic enthusiasm, inspired me to pursue my passion for science and engineering.*

*Dr. Woong-Jae Boo who has assisted me in passing through various obstacles in life and academia, while extending friendship beyond limits.*

## TABLE OF CONTENTS

	Page
ABSTRACT .....	iii
DEDICATION .....	v
TABLE OF CONTENTS .....	vi
CHAPTER	
I INTRODUCTION.....	1
Significance of Scratch Study .....	1
Overview of Scratch Research .....	3
Thesis Layout .....	8
II EFFECTS OF MOLECULAR WEIGHT AND THERMAL HISTORY ON SCRATCH BEHAVIOR OF POLYPROPYLENE THIN SHEETS .....	9
Introduction .....	9
Experimental .....	12
Results and Discussion.....	16
Conclusion.....	34
III SCRATCH BEHAVIOR OF EPOXY BASED NANOCOMPOSITES: EFFECTS OF ADDITIVES OF VARIOUS NATURES.....	35
Introduction .....	35
Experimental .....	39
Results and Discussion.....	43
Conclusion.....	55
IV CONCLUSIONS AND REMARKS.....	57
Conclusions on PP Study .....	58

	Page
Conclusion on Epoxy Study .....	59
Conclusions on Failure and Material Nature.....	60
Conclusions on Effective Parameters.....	60
Recommendations for Future Work.....	61
REFERENCES .....	62
VITA .....	68

## LIST OF FIGURES

FIGURE		Page
1	Scratch research progress over recent years.....	3
2	Consideration factors for scratch studies .....	5
3	Schematic of a scratch process.....	6
4	Scanned images after j-image processing for all four PP systems .....	17
5	Critical load values for onset of scratch visibility.....	17
6	SCOF of (a) HA vs. HQ & (b) LA vs. LQ .....	19
7	SCOF of (a) HA vs. LA and (b) HQ vs. LQ .....	20
8	Optical micrographs of scratch cross-sections illustrating skin-core morphology in (a) HA (b) HQ (c) LA and (d) LQ .....	22
9	DSC plots of the PP systems .....	24
10	OM of Mar/Scratch and Scratch/Severe Damage transitions in (a) HA (b) HQ (c) LA and (d) LQ.....	25
11	Scratch hardness measurements for studied systems .....	27
12	Subsurface damage observed along scratch direction for (a) HA and (b) LQ systems .....	30
13	A schematic of fish-scale pattern formation .....	31
14	Scanned images of scratched surfaces of an injection-molded TPO specimen subject to different processing conditions .....	33
15	Critical load for the onset of scratch visibility for an injection-molded TPO specimen subject to different processing conditions .....	33
16	Optical micrographs of onset of macro-crack formation .....	44



FIGURE	Page
17	Critical normal load values for onset of damage..... 44
18	SCOF comparison of three systems ..... 45
19	Tangential load values along the scratch path..... 46
20	Longitudinal cross sections of scratch valley at the onset for macro-crack formation ..... 48
21	Evidence of secondary crack formation shown by optical microscopy ..... 49
22	SEM images of CSR ..... 50
23	SEM images of ZRP..... 50
24	Optical micrographs of mar transition ..... 51
25	SEM images of various observations in mar region ..... 52
26	Surface roughness profiles before and after mar transition for (a)NE (b)ZRP and (c)CSR..... 54
27	Surface roughness profiles in the longitudinal direction for (a)CSR and (b)ZRP ..... 55

## LIST OF TABLES

TABLE		Page
1	Material specifications for as-received PP systems .....	12
2	Degree of crystallinity for skin region of PP systems .....	22
3	Composition of epoxy systems .....	40
4	Physical and mechanical properties of systems .....	47

# CHAPTER I

## INTRODUCTION

In this chapter, preliminary remarks are made to highlight the significance of scratch research and review the development of this area in the past. Important factors and considerations which set the limitations of scratch study are evaluated in detail to give an appreciation of the inherent complexity in research. Finally, an outline is provided to lay out research components and the order which they will be evaluated upon in this thesis.

### **SIGNIFICANCE OF SCRATCH STUDY**

Aesthetics and high quality appearance is a determining attribute which both industrial manufacturers and product consumers aspire for various products. While obtaining a satisfying finished surface of quality creates a challenge for manufacturers, the sustainability of the quality related to the surface throughout its service life has been shown to construct of the bigger challenge to overcome.

For polymeric materials, the major surface quality concerns can be grouped into aestheticism (appearance), overall integrity, and long-term durability. For surface aestheticism concerns, little thought is needed to recognize numerous applications which will be affected by this aspect such as cellular phones, car stereo panels, dashboards, etc.

---

This thesis follows the style of *Tribology International*.

For such products surface scratches simply result in loss of attractiveness for the product while mainly not affecting the function and use of the equipment. On the other hand applications such as packaging of food and drugs, require surface integrity of the packaging materials as a necessity and surface scratches could cause complete malfunction in that application and therefore is of significant importance. Scratches formed on packaging materials (films, coatings, etc.) can initiate tearing, which may lead to the products loss of value and destroy. However surface durability is the major concern for industrial manufacturers of products such as coatings and electronics. Scratch damage will result in serious consequences for these products, i.e. exposed surfaces due to coating failures may lead to corrosion or damage of the protected substrate, while a scratch on a hard disk drive, optical storage device (such as CDs), or memory cards can result in the loss of considerable data resources as well as valuable labor required to produce the device. Therefore, coatings are desired to remain intact for the service life of the product and materials utilized in the electronic industries are required to resist scratch deformations to a certain extent.

The main disadvantage caused by a scratch deformation that has not been adequately considered in previous research efforts is the stress concentration effect resulting from the formation of the scratch. This stress concentration factor can cause the related product to eventually fail in a premature fashion which premature fracture can be attributed to this effect. The neglected premature failure can result in catastrophic out comings.

## OVERVIEW OF SCRATCH RESEARCH

Based on the previous discussions the significance of scratch research for industries is completely evident. However, the concern for surface damage and defects in polymeric applications had not been significantly considered until a few decades ago, but today the progresses in polymer science and engineering have assisted growth in this area. A schematic of this fact can be seen in Figure 1. It can be seen that although the number of research publications related to this area were minimal before the 1980s, recently the emphasis on scratch study has been shown by the substantial increase in scientific studies.

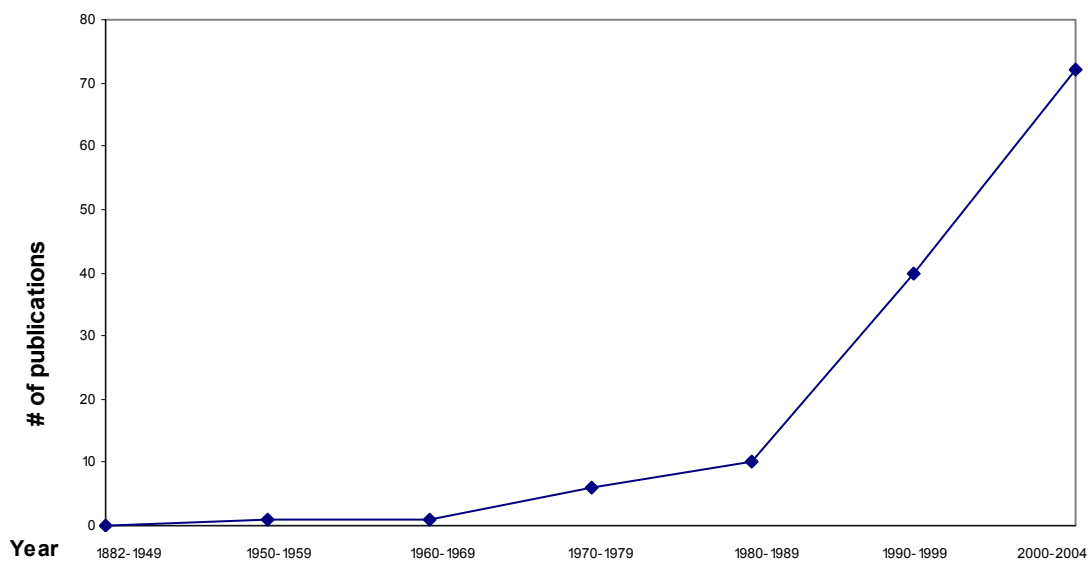


Figure 1 Scratch research progress over recent years

Due to widespread applications of metals and ceramics in various applications prior to the introduction of polymeric materials, these traditional materials and their response to scratch deformations have been previously examined. In the case of polymers there are various factors that have limited the thorough evaluation of scratch performance and caused slow progress in this area. On one hand polymer scratch is a relatively new research area, while the lack of a universally excepted standardized test method up until just a few years ago has caused complications. Previously developed testing standards for scratches in ASTM [1] and ISO [2-3], are younger than 10 years, which are known to be more applicable to ceramics and mar studies, respectively. The lack of a standardized scratch testing methodology caused researchers to each develop testing equipments and methodologies limited to specific studies, which were the basis for scratch evaluation and study by the examiner. An adequate list of scratch equipment used by various researchers in the past can be found in a publication by Lim et al. [4]. Based on the lack of consistency in testing equipments and conditions, the findings of previous studies can be subjective.

On the other hand, the scratch evaluation parameters and quantification tools has also varied from one researcher to another, ranging from the subjective human eyesight to more objective tools such as optical scanners. These limitations in scratch testing and evaluation adversely lead to a complicated situation for researchers which have either been incapable to generate highly repeatable results or unable to verify experimental results. As expected these factors will hinder progresses in scratch studies.

In order to gain insights on the fundamentals of scratch resistance of polymers and make an effort to correlate the material properties of the polymer to the scratch behavior it is necessary to fully explore the material science as well as physics and mechanics aspects of the problem as well as any possible interactions of these aspects. Figure 2 is an example of a list of inevitable considerations and factors that must be taken into account during scratch studies. This itself is an indicator of the level of complexity encountered in an effort to perform fundamental studies on scratch resistance of polymers

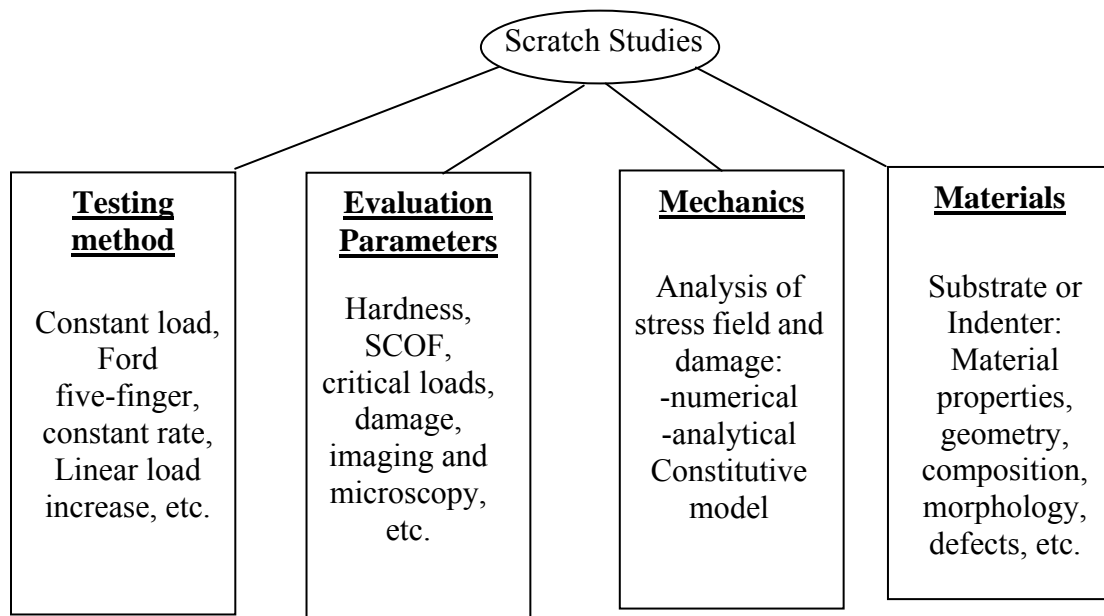


Figure 2 Consideration factors for scratch studies

The complexities of the induced stress field and resulting deformation in a scratch process cause the material's physical and mechanical response to depend on factors such as tribology, type of analysis, material damage and analysis technique. Surface

interaction between the indenter (scratch tip) and scratched material (substrate) during a scratch process results in friction which itself generates heat. The simplest model that can be used to correlate the frictional force ( $F$ ) and normal load ( $N$ ) upon the surface is Coulomb's friction model [5]. This model considers a constant coefficient of adhesive friction ( $\mu_a$ ) and is shown below:

$$F = \mu_a \times N$$

Figure 3 is an illustration of an indenter as it pushes into the scratch surface due to a controlled normal force or displacement, and traverses across the surface. It can be seen that after the scratch tip moves along the surface the indenter not only interacts with the top of the substrate's surface, it also comes into contact with the sub-surface and core of the substrate with the exposure of underlying materials from scratch damages. This introduces additional complexities to the study as the coefficient of adhesive friction does not correctly account for the frictional property of the sub-surface and core of the material. It is to be expected that portions of the scratch which have ruptured will demonstrate a noticeable increase in surface roughness, resulting in higher frictional forces as well.

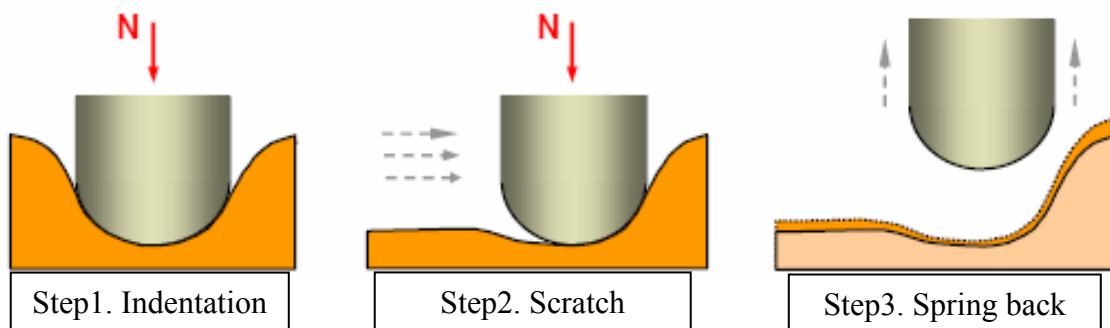


Figure 3 Schematic of a scratch process



In terms of material scope, scratch studies should have the ability to analyze different behaviors such as non-linear elasticity, viscoelasticity, and etc. and predict scratch response based on material properties as well as these factors in a material. As scratch deformations may extend beyond the material's yielding criteria, scratch analysis should be able to consider possible plastic deformations.

The next crucial issue in the evaluation of scratch is to have an adequate description of the damage induced on polymers. It is well-known that polymers, when subjected to a stress field and hence deformed, can yield in shear or undergo crazing/cracking, depending on the type and extent of deformation. The fact that these two failure modes can coexist together, even though there may be a dominant mechanism between the two further complicates the damage prediction. During a scratch process, induced stress fields on the material can alter drastically from tension to compression as the indenter plows across the substrate as shown in previous studies. The treatment of material damage becomes more challenging for polymer composites since the composite can be layered, *e.g.*, coated system, or particulated, *e.g.*, rubber-modified polymers. Depending on the adhesive strength between the matrix and fillers, delamination or cavitation may occur locally at the interfaces.

In this study polypropylene and epoxy were chosen due to the different types of mechanical behavior they demonstrate, as PP usually shows ductile or semi-ductile behavior and epoxies normally behave in a brittle or semi-brittle fashion. Therefore these materials are adequate in order to further investigate the various fracture and failure mechanisms caused by a scratch process and the dependency of the failure on various

material properties such as molecular weight, degree of crystallinity, etc. Furthermore, the mar region was further investigated and a new insight on the nature of the mar transition has also been provided based on recent findings.

## **THESIS LAYOUT**

As mentioned earlier, two experimental studies were examined separately and combined in this thesis. In the study outlined in Chapter II, a set of PP thin sheets of high and low molecular weight were quenched and gradually cooled after being annealed. Comparisons of the scratch response of the high and low MW sheets as well as quenched and gradually cooled samples lead us to some assumptions which based on further experimental analysis can be concluded. In Chapter III, a similar scratch evaluation is performed on a set of epoxy composites. The systems utilized for the study indicated in Chapter III were epoxy (DER-332) nanocomposites containing CSR nanoparticles or  $\alpha$ -ZrP nanoplatelets as well as the neat system. Based on the scratch damage observed in these epoxy nanocomposites and the findings of previous studies including their mechanical properties, results of this section were explained. Concluding remarks to summarize the findings of this research and recommendations for future related studies to be carried out are given in Chapter IV. Finally in the last chapter (Chapter V), citation of referred literature in the dissertation is documented. Derivations and results, that are non-essential but complementary to the chapters, are collected in the appendices of the thesis.

## **CHAPTER II**

### **EFFECTS OF MOLECULAR WEIGHT AND THERMAL HISTORY ON SCRATCH BEHAVIOR OF POLYPROPYLENE THIN SHEETS**

The effects of molecular weight (MW) and thermal history on the scratch behavior of polypropylene (PP) thin sheets and a model thermoplastic olefin (TPO) have been investigated. Scratch parameters, such as the critical load for onset of scratch visibility, scratch coefficient of friction, and scratch hardness, were utilized in this evaluation. The results suggest that scratch performance is improved when the MW and surface crystallinity of PP are high. Correlation between scratch resistance and surface morphology of PP is established and discussed. Approaches for preparation of scratch resistant TPOs are also addressed.

#### **INTRODUCTION**

Scratch behaviors of metallic and ceramic materials have been widely explored since the 1950's [6,7]. However, fundamental scratch behavior of polymeric materials has not been the focus of significant research until about a few years ago [8-15]. Now, owing to the widespread uses of plastics in durable goods applications, and especially due to their soft surface nature, the scratch behavior of plastics has drawn significant attention in recent years.

Previously, attempts to systematically quantify the scratch resistance of polymers have been problematic due to the lack of a general test standard and appropriate evaluation tools. The scratch resistance of a material had previously been defined as the ability of a material to withstand abrasion with another body [16,17]. Most recently, Sue et al. have developed a new standard test methodology, ASTM D7027-05, for evaluating scratch resistance of polymers and coatings [18,19]. The standard methodology consists of a linear load increase test and a set of well-defined scratch evaluation parameters, such as scratch visibility, depth, width, and hardness. Using this methodology, consistent and highly repeatable results have been attained.

Through the detailed examination of the scratch behavior of plastics, it has been shown that the scratch behavior of plastics depends on various parameters [11], such as scratch loads and speeds [20-22], coefficients of friction [8,20-22], geometry and number of scratch tips [8,20-22], and types and amounts of fillers and additives incorporated [23-25]. In addition, material properties will also definitely have an impact on the scratch behavior of plastics. In our previous studies, rudimentary investigations and discussions have been made on how elastic modulus, yield stress, tensile strength, coefficients of friction, and viscoelastic recovery affect scratch behavior of polymers [8,13,25]. More careful and systematic experimental studies are still needed.

Another set of parameters that has a significant effect on material properties, and therefore must be considered, are processing and molding conditions. In injection molding and extrusion of semi-crystalline polymers, the melt cooling rate and mold temperature will definitely play an important role in determining the physical and mechanical

properties of the molded article. Generally, plastics are poor heat conductors, which contributes to the formation of a so-called skin-core morphology during molding, where a gradient of molecular orientation, density, and crystallinity develops from the skin toward the core of the molded part. The thickness of the skin depends strongly on the mold temperature, cooling rate, and the use of nucleation agent [26,27].

Many approaches are known to be effective in controlling the skin-core morphology as examined elsewhere [28]. For example, a higher overall cooling rate and a higher molecular weight (MW) will result in an increase of skin thickness. The skin and the core are expected to have different physical and mechanical properties [28]. Thereby, variation in skin-core morphology is expected to strongly affect scratch behavior of polymers.

Polypropylene (PP) is one of the most utilized commodity plastics today because of its good combination of properties and low cost. However, some disadvantages may limit its use, namely, its poor low-temperature impact strength, surface crazing upon repeated flexing, scratch resistance, etc. [28]. Furthermore, as the mechanical properties of PP are known to be greatly influenced by the processing conditions [28,29], especially in the case of injection molded pieces [30-32] or after heat treatments such as annealing [33,34], it is an ideal material to investigate the influence of processing, which, in turn, causes surface morphology variations, on scratch performance of plastics.

In this study, the effects of skin-core morphology differences on scratch behavior are explored for two model PP systems having two different molecular weights (MW). Various scratch parameters for evaluation will be examined and discussed. The above

findings will also be correlated with the scratch behavior of a thermoplastic olefin (TPO) system where different injection molding mold temperatures were also varied. The usefulness of varying MW and mold temperatures to prepare scratch resistant PP will be discussed.

## **EXPERIMENTAL**

### *Materials*

Specimens of injection molded PP with two different MWs were obtained from the Dow Chemical Company. The MW, tacticity, and melt flow rate of the systems are listed in Table 1.

Table 1 Material specifications for as-received PP systems.

System	M <sub>w</sub> (g/mol)	MFR	Tacticity	Thickness
HA	416,000	1.5	98.5%	1mm
HQ				
LA	305,000	4.5	98.5%	1mm
LQ				

Four systems were examined: high MW gradually cooled (HA), high MW quenched (HQ), low MW gradually cooled (LA), and low MW quenched (LQ). The dimensions for all of the samples were 124mm x 124mm x 1mm.

In addition, a model TPO system containing 78 wt% PP/ethylene-propylene-rubber (PP/EPR), 20 wt% talc filler and 2 wt% carbon black pigment were obtained from Advanced Composites. The TPO was injection-molded into 80 mm by 160 mm by 3 mm plaques where the temperature of the mold wall was held at 26.7 °C (80°F), 37.7 °C (100°F) and 48.9 °C (120°F).

#### *Heat Treatment*

Annealing was carried out at 140°C for 30 min on PP systems followed by gradual cooling or quenching. The procedure took place in a Napco E5851 vacuum oven. The gradually cooled samples were cooled at a rate of 0.5°C/min to room temperature. The quenched samples were immediately cooled down to 0°C by directly immersing the specimens into an ice bath.

#### *Scratch Testing*

A recently developed standardized test method, ASTM D7027-05, was used for the scratch testing of the samples. A constant scratch speed of 100 mm/s with a load range of 1-50 N was used for a scratch length of 100mm for the PP; whereas the load range for the TPO systems was only 1-30N to enhance resolution for observing the critical loads for scratch visibility. The tests were performed at room temperature using a stainless steel spherical shaped scratch tip with 1 mm in diameter. The scratch directions for the testing were all oriented in the direction of the melt flow to prevent variation in scratch damage due to possible orientation effects. A minimum of 5 tests were performed per sample.

### *Scratch Damage Quantification*

After the scratch tests were performed, the samples were scanned using an Epson 4870 perfection scanner at 3,200 dpi under the 8-bit grayscale mode. The scanned images showing the scratch on each sample were evaluated using an image-J program grayscale threshold function. This function enhances the contrast between the scratch damaged region and the undamaged region leading to a simple quantitative determination of the location for the onset of scratch visibility. After measuring the distance of this onset point ( $x$ ) from the initial point, the critical load for scratch visibility can be calculated by a simple interpolation of the two end loads:

$$F_C = \frac{x}{L}(F_e - F_i) + F_i \quad (1)$$

where  $F_C$ ,  $F_i$ ,  $F_e$ , and  $L$  are the critical load, initial load, end load, and scratch length, respectively.

### *Scratch Coefficient of Friction*

The scratch coefficient of friction (SCOF) is defined as the ratio of the tangential force to the normal force at each loading point. The scratch testing instrument utilized in this study is capable of *in-situ* determining the actual normal and tangential force at each point of the scratch which results in SCOF:

$$SCOF = \frac{F_z}{F_x} \quad (2)$$



### *Scratch Hardness*

Scratch Hardness is defined as the normal load of the indenter over the projected load bearing area. It is normally taken to be equivalent to the indentation mean pressure exerted on the material during scratch [13]. Thus, scratch hardness,  $H_s$ , can be expressed as:

$$H_s = \frac{4W}{\pi d^2} \quad (3)$$

where  $W$  and  $d$  are the normal load and the residual scratch width, respectively. The scanned images were processed by a contrast inversion followed by the adjust/equalize function of Adobe Photoshop to show a higher contrast between the scratched and the non-scratched region. On each scratched sample, 9 points were selected at 10, 20, 30, ..., 90 mm from the starting point of the scratch. The pixel to pixel distance of the two sides of the scratch were measured and converted into the scratch width considering the scanning resolution (3,200 dpi). The load at that point can be calculated simply by using the previous equation for critical loads with values of  $x=10, 20, \dots, 90$ .

### *Optical Microscopy Observation of Scratch Damage*

In order to determine the differences in the skin-core morphology of the different PP systems, cross-sections of the scratch were examined. All cross-sections were taken at the location of the scratch which had a normal load equivalent to  $F=37.5\text{N}$ . Longitudinal-sections along the scratch direction were also examined to determine the subsurface damage for the best performing and the worst performing systems, i.e., HA and

LQ, respectively. Top view images were taken to determine the scratch transitions. The microscopy images were captured using an Olympus BX60 optical microscope under cross-polarized as well as bright field conditions.

#### *Differential Scanning Calorimetry*

Differential scanning calorimetry (DSC) was performed using a Mettler Toledo DSC821 from 25°C to 190°C using a heating rate of 5°C/min with nitrogen as the purge gas (80mL/min). In order to examine the crystallinity of the skin region, top layers with a thickness of about 100 µm were carefully separated from the samples for DSC analysis.

## **RESULTS AND DISCUSSION**

The processed scanning images of the scratches of the scratched samples are shown in Figure 4. Comparing between the gradually cooled and quenched PP systems (HA vs. HQ and LA vs. LQ), the resistance to scratch visibility is better for the gradually cooled systems. Furthermore, the comparison between the low MW and high MW systems (HA vs. LA and HQ vs. LQ) displays a delay in the critical load for scratch visibility for the high MW system. These observations are quantitatively reported in Figure 5.



Figure 4 Scanned images after j-image processing for all four PP systems.

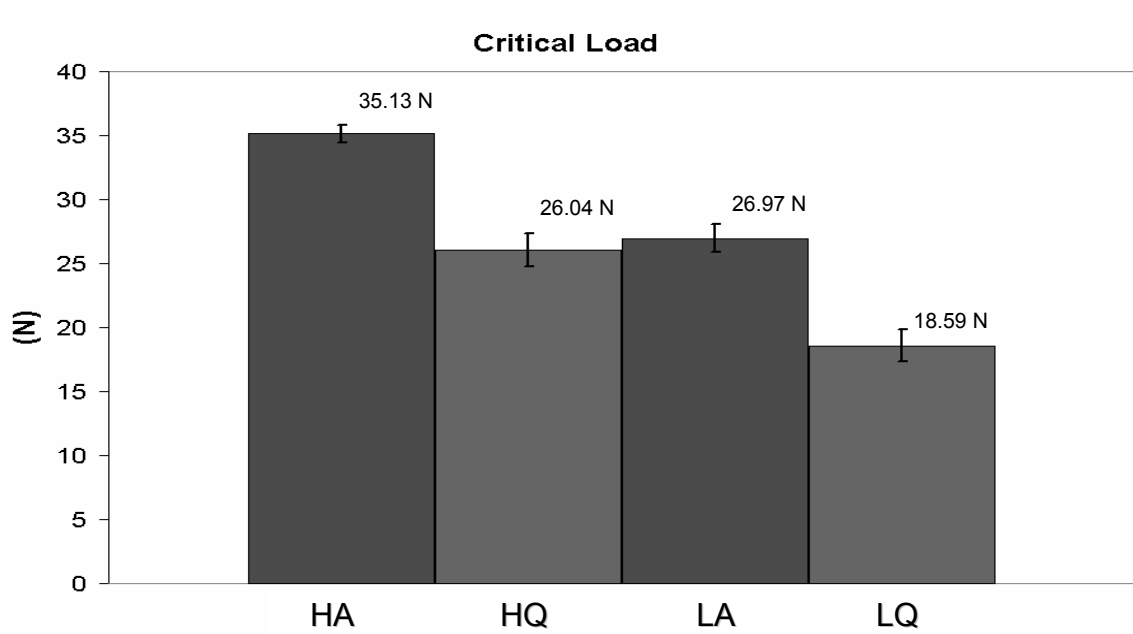


Figure 5 Critical load values for onset of scratch visibility.

The SCOF of the gradually cooled and quenched PP systems are shown and compared in Figure 6. It is obvious that in both high and low MW systems, the SCOF for the gradually cooled systems is lower than that of the quenched systems, indicating that at similar normal loads the tangential load (i.e., frictional force) corresponding to the gradually cooled systems is lower compared to the quenched systems. Figure 4 shows the SCOFs of the high MW systems in comparison to the low MW systems. It is evident that in both quenched and gradually cooled cases, the low MW systems show a higher SCOF than the high MW systems.

It can be seen that the critical load for scratch visibility and SCOF show similar trends between systems. The trend suggests that lower SCOF will result in a higher critical load for scratch visibility. In Figures 6 and 7, it is also observed that the difference in SCOF between the systems decreases at higher loads and eventually the SCOF of all the systems become equivalent. Hence, it can be interpreted that beyond a certain normal load, which causes a certain scratch depth in the sample, the SCOF becomes independent of the skin-core morphology of the samples. This scratch depth (or the critical load) occurs after the critical load for scratch visibility in all of the PP systems.

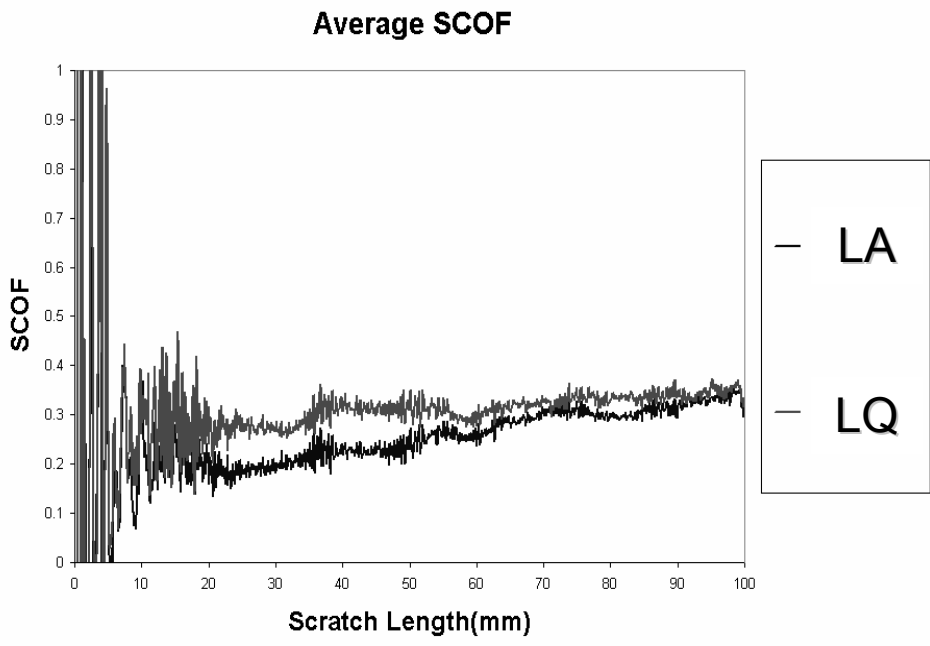
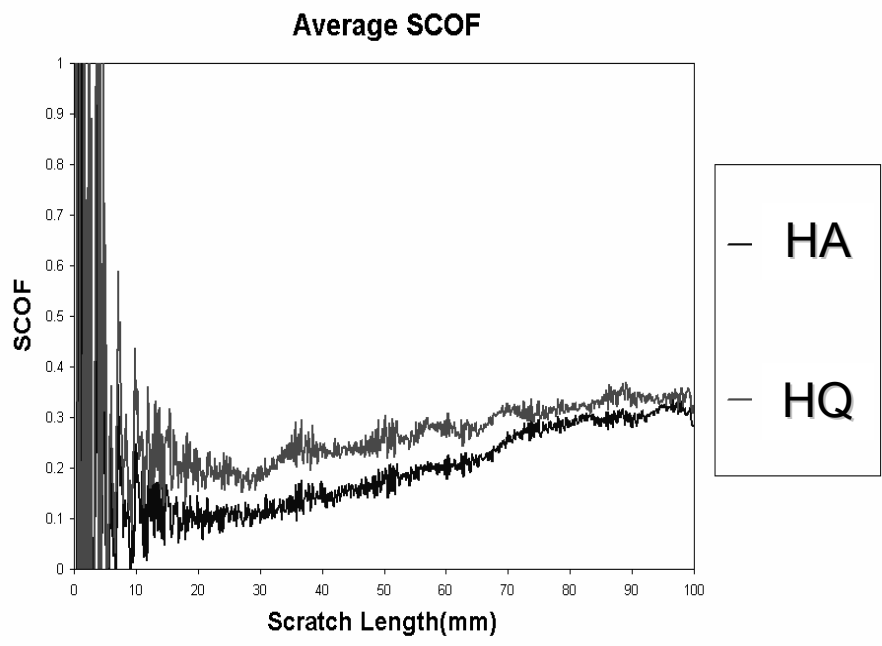


Figure 6 SCOF of (a) HA vs. HQ & (b) LA vs. LQ.

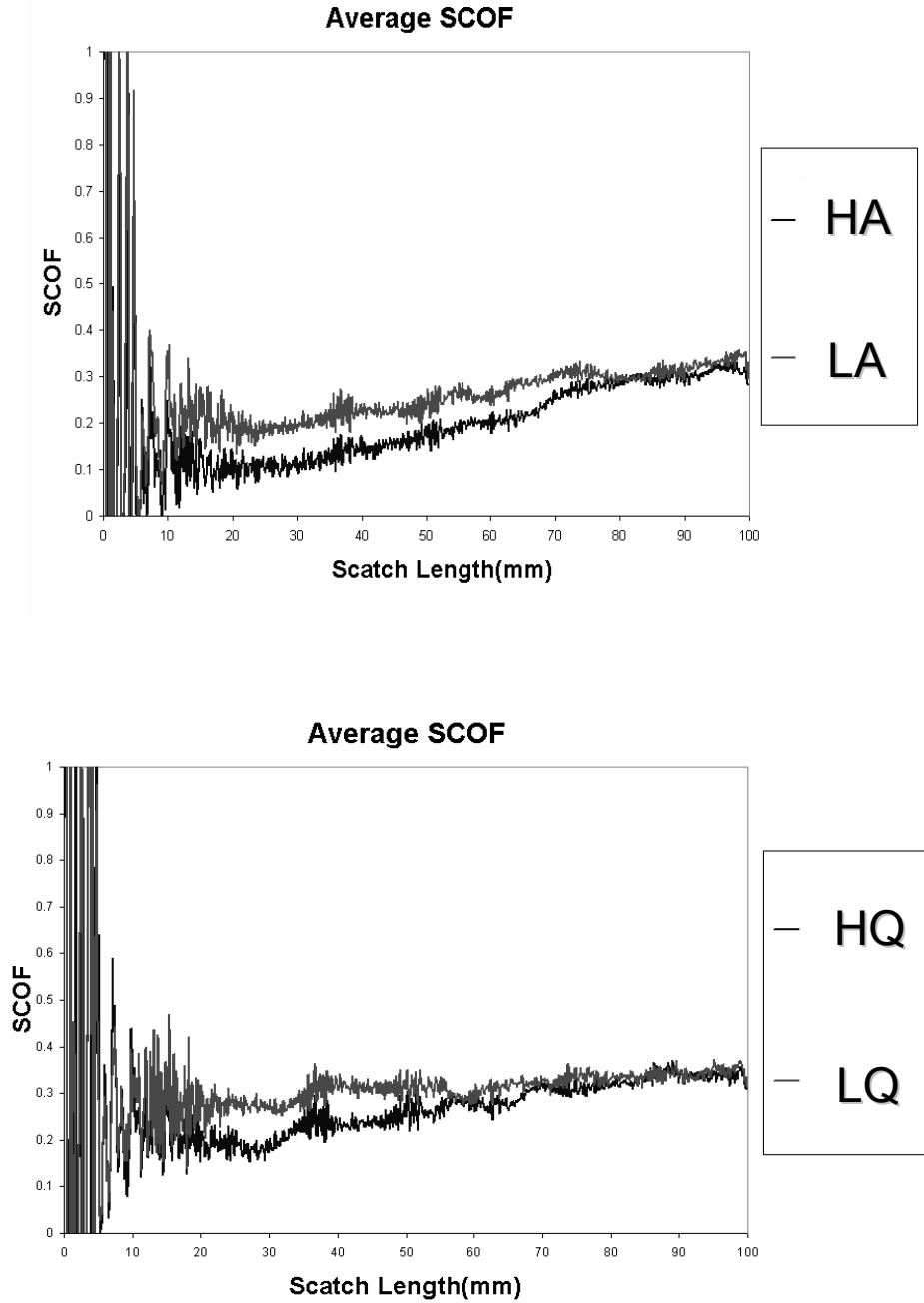


Figure 7 SCOF of (a) HA vs. LA and (b) HQ vs. LQ.

The effects of post-processing cooling rates on various mechanical properties of semi-crystalline plastics have been investigated in previous studies [26,34-37]. It has been shown that variation in cooling rates can result in variations in the skin thickness observed in the skin-core morphology of the plastic. This variation will definitely have a major influence on the mechanical properties of the samples due to the lower crystallinity of the skin region. Thus, it is expected that the scratch resistance of PP will be greatly altered if the surface mechanical properties are changed, as have been observed in this study.

In order to further substantiate the above claim, attention can be drawn to the observed skin-core morphology of the samples in Figure 8. It can be seen that in both cases the skin thicknesses for the gradually cooled samples are significantly less than those of the quenched samples. Furthermore, a crystallinity comparison between the skin layers of the quenched and gradually cooled systems would give a more direct account on the enhanced scratch properties of the gradually cooled systems. The DSC results shown in Figure 6 are a good example of such a comparison. It is obvious that the crystallinity of the skin layers for the quenched samples are much lower than that of the gradually cooled samples.

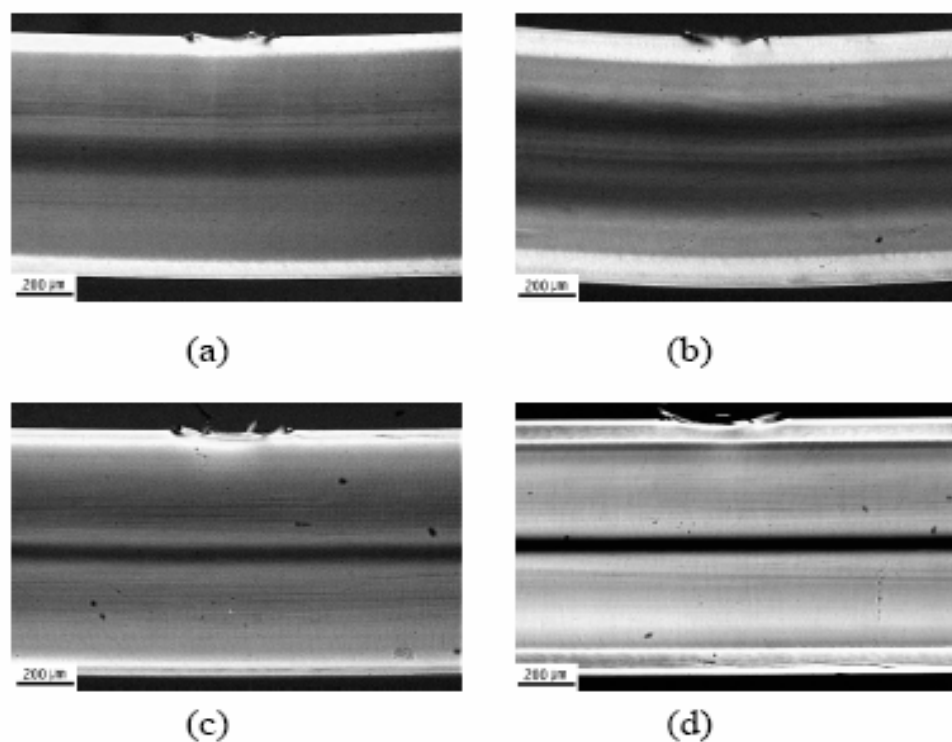


Figure 8 Optical micrographs of scratch cross-sections illustrating skin-core morphology in (a) HA (b) HQ (c) LA and (d) LQ

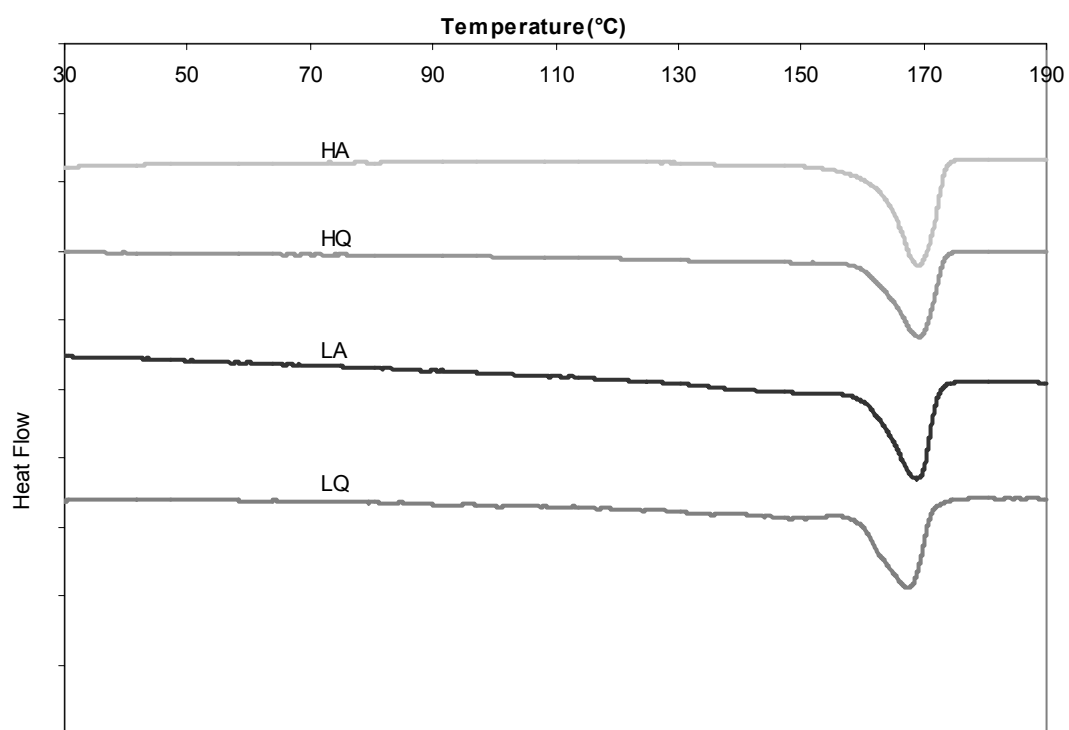
Table 2 Degree of crystallinity for skin region of PP systems.

Sample	Crystallinity %
HA	46.05%
HQ	36.31%
LA	40.16%
LQ	34.80%



The skin layer crystallinity results of the four PP systems are quantitatively reported in Table 2. It can be observed that the skin crystallinity of the gradually cooled systems are approximately 5-10% higher than that of the quenched systems. Therefore, the observed increase in the critical load for scratch visibility of the gradually cooled systems compared to the quenched systems can be attributed to this increase in the crystallinity of the skin region in which the scratch tip has ploughed through. This increase in skin crystallinity will also reduce the frictional force between the scratch head and the skin region (Figure 6).

The variation in MW has also been shown to have a significant effect on various mechanical properties of semi-crystalline polymers [38-44]. The increase in MW has shown to be effective on enhancing mechanical properties, such as yield stress, elongation at break, and tensile strength of the polymer. However, the increase in MW for a given system will also lead to reduced molecular mobility for crystallization. In order to compare the skin-core morphology of the high MW and low MW systems, attention can be drawn to Figure 8 which illustrates the relative skin thickness of the systems. It is apparent that the skin thickness for high MW is higher than that of the low MW for both quenched and gradually cooled cases. The higher mobility of the polymer chains for the low MW can be a reason causing the decrease in skin thickness as this claim can also be supported by its higher melt flow rate (Table 1).



DSC Micrographs

Figure 9 DSC plots of the PP systems.

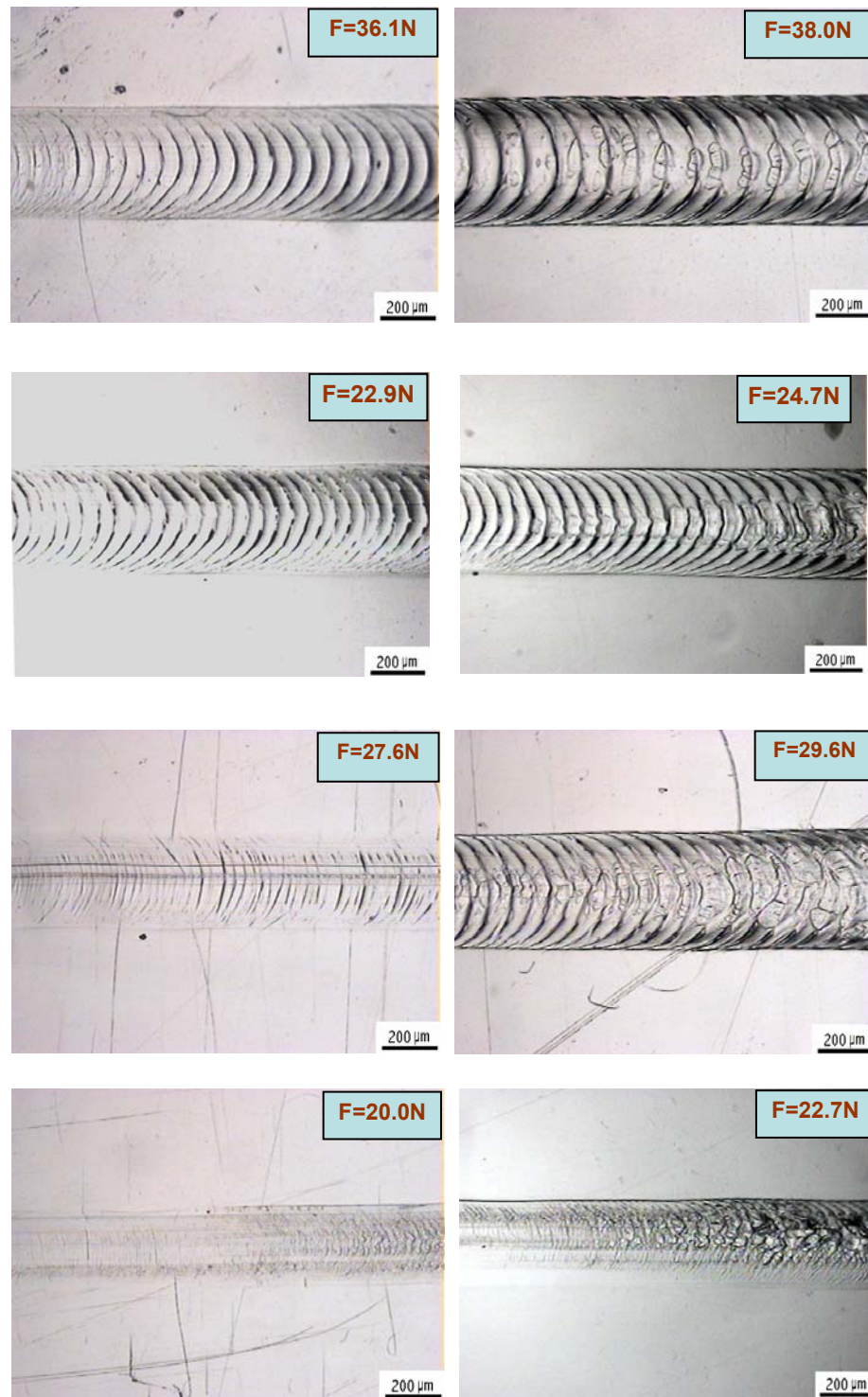


Figure 10 OM of Mar/Scratch and Scratch/Severe Damage transitions in (a) HA (b) HQ  
(c) LA and (d) LQ.

Nevertheless, unlike the comparison between different cooling rates, a lower skin thickness does not necessarily result in a higher crystallinity. As shown in Fig. 9 and Table 2, the DSC results show that, at similar cooling rates, the crystallinity in the skin region of high MW is higher than low MW systems. However, in this case not only is the skin layer affected by the property enhancements due to the crystallinity increase, MW itself has also had a major influence on the mechanical properties. The enhancement in mechanical properties due to MW increase is likely to improve the PP ductility and strength, which have been shown to be critical for improving scratch resistance [8]. Therefore, the delay in the critical load for scratch visibility of the high MW systems can be explained by the enhanced mechanical properties and the lower frictional force between the scratch tip and the skin region, partially because of the increased crystallinity.

Figure 7 shows the SCOF of the high MW and low MW systems at both cooling rates. The observed decrease in SCOF for the high MW systems can also be explained by the less scratch tip penetration into the skin region. It can also be observed that after a certain scratch depth and normal load, the SCOF is no longer a function of MW and the skin-core morphology as the scratch tip has penetrated through a certain scratch depth.

The scratch damage mechanisms and mar/scratch and scratch/severe damage transitions along the scratch direction for all four systems are shown using OM (Figure 10). The locations of the transitions and the corresponding normal loads for the transition are shown. It can be seen that, independent of the PP systems, the scratch damage feature after the scratch/severe damage transition are the same for all systems independent of their skin-core morphology. As expected, it is also observed that the trend for the location of the

mar/scratch transition for the systems is similar to the trend for their critical loads for scratch visibility.

Furthermore, comparison of the scratch transitions between the systems leads us to the conclusion that in the case of high MW and gradually cooled systems, the fish-scale pattern is more evident on the scratch path. The main reason behind the more regular fish-scale pattern can be the higher ductility of the HA system as compared to the LQ as has been shown for PP systems in our previous studies [26-29].

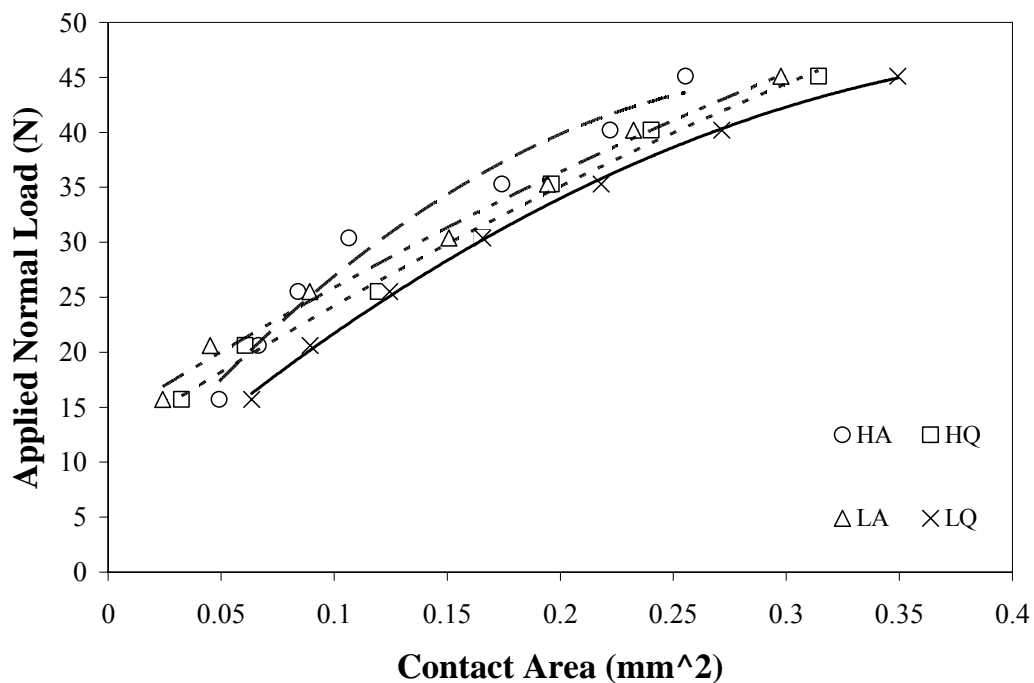


Figure 11 Scratch Hardness measurements for studied systems.

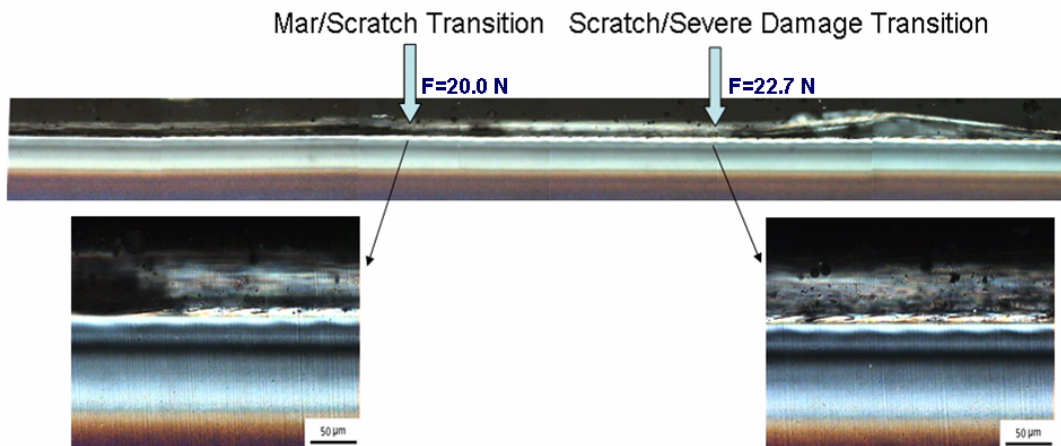
To obtain scratch hardness values,  $H_S$ , the normal loads against projected contact area is plotted in Figure 11. The average slope for each of the fit lines represents the scratch hardness for that set. The fit curves illustrate a deviation from linearity between the applied normal load and the contact area. As demonstrated elsewhere [8-12], the scratch hardness of a system is highly dependent on the modulus and elastic recovery of the material, types and amount of additives to the system, and the skin layer morphology. In this case, due to the similarity in the slopes of Figure 11, it seems that the scratch hardness is not noticeably dependent on the cooling rate and MW of PP. The apparent nonlinearity of the curves in Fig. 11 clearly indicate that  $H_S$  is not a constant for the PP systems. In other words, the  $H_S$  values varies with the applied load, and hence the scratch depth. The nonlinearity of the curves can possibly be explained by the scratch tip geometric effect and the variation of mechanical properties of the skin-core morphology. In this case, due to the relative decrease in the scratch hardness under progressive loading, it seems the geometric effect plays more of a dominant role. Therefore, scratch hardness is not a useful parameter to characterize scratch resistance unless a fixed load is assigned for the measurement. Also, since scratch visibility is more relevant to the scratch-induced surface damage feature generated,  $H_S$  would not be able to physically correlate with scratch visibility [14]. Only when the surface damage mechanisms are the same among the systems to be compared will the  $H_S$  be useful for ranking scratch resistance against visibility.

In order to investigate the subsurface damage caused by the scratch, longitudinal sections along the scratch direction have been examined for the two extreme cases in

Figure 12. It can be observed that in both cases the mar/scratch and scratch/severe damage transitions are evident by the similar types of subsurface damage caused by the normal and frictional force acting upon that region of the material. However, the damage pattern is more evident and severe for HA when compared with LQ. This fact is due to the higher normal load at which HA reaches the transitions. In other words, for LQ the critical load for scratch visibility and thus the mar/scratch transition occurs at a normal load of  $F=18.5\text{N}$ ; while this transition in the case of HA occurs at  $F=35.1\text{N}$ , which is almost twice the normal load accrued than the previous case.

Furthermore, the longitudinal section along the scratch direction of the scratched samples can also illustrate that the type of damage and fracture mechanisms caused by the scratch tip. The apparent microcracking observed is evident at the edge of each fish-scale which is due to the combined tensile drawing, followed by compressive ironing of the PP on the surface. For clarity, a schematic showing how a fish-scale pattern during scratch is formed is shown in Fig. 13.

## Sample LQ



## Sample HA

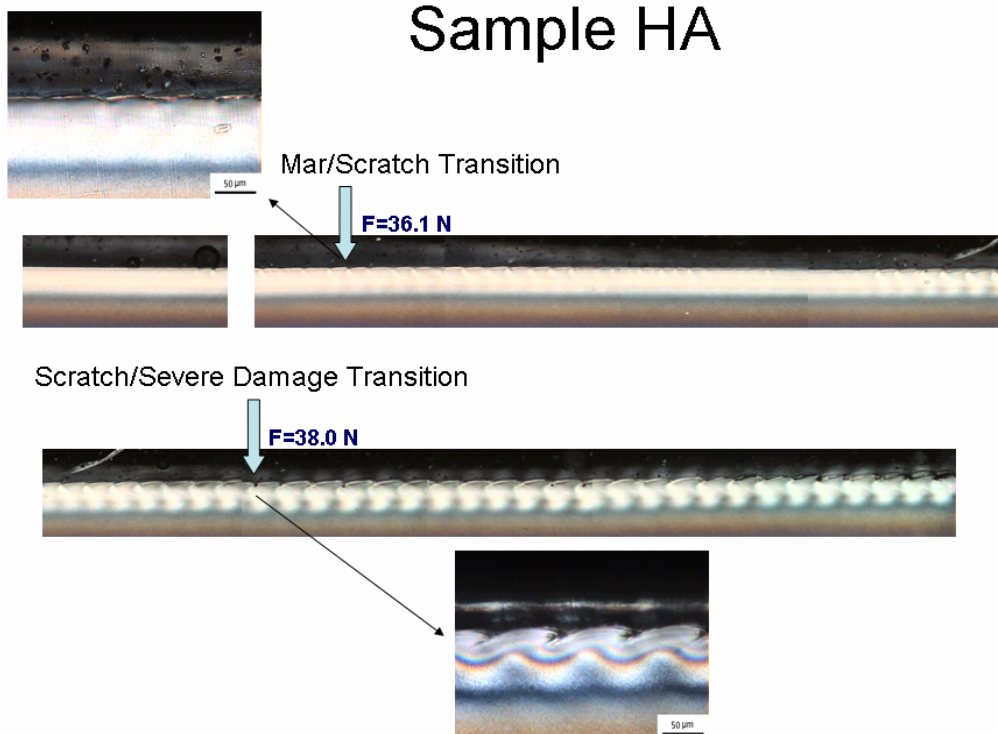


Figure 12 Subsurface damage observed along scratch direction for (a) HA and (b) LQ systems.



Understanding the fundamental scratch behavior discussed above using a model PP is essential. In the case of industrially relevant TPO systems, which contain rubber, fillers, and other additives, it is uncertain whether or not the fundamental knowledge gained above can be applied to a typical commercial TPO system. To illustrate the relevance of the above fundamental study with a complex commercial TPO system, a typical TPO system was molded at 26.7 °C (80°F), 37.7 °C (100°F) and 48.9 °C (120°F) to study if indeed mold temperatures, which affects the cooling rate of TPO, can greatly affect the scratch behavior of TPO. Figure 14 shows the scanned images (,3200 dpi resolution) of the scratch surfaces. Figure 15 shows the corresponding values of critical load of onset of scratch visibility for the three TPO specimens.

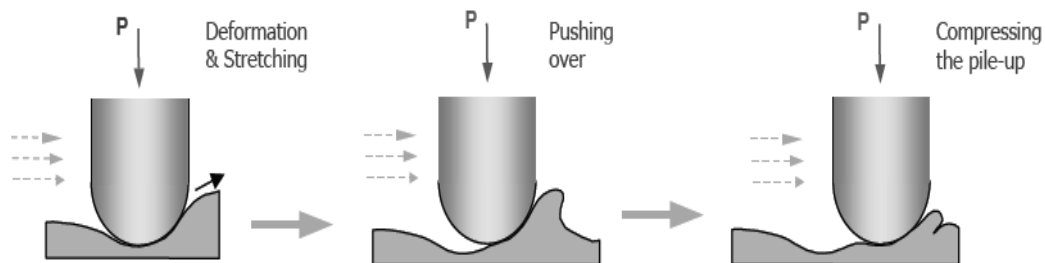


Figure 13 A schematic of fish-scale pattern formation

From the above results, it is readily observed that the TPO exhibits an increase in scratch resistance as the mold wall temperature is increased. This is analogous to the trend seen in the behavior of the model PP systems. When the TPO is quenched, or when the mold wall is held at a low temperature, there is a large temperature gradient between the polymer and the mold wall, resulting in rapid cooling. The converse is true for the case of

slowly cooled PP (or holding the mold wall at a higher temperature in the injection-molded case). It is noted that attempts were made to investigate the skin-core morphology of the TPO system using OM and DSC. However, the presence of the talc filler and EPR tended to convolute the results so that the skin-core morphology could not be clearly discerned.

The above findings on TPO are in excellent agreement with the model PP systems observed. In other words, a slowly cooled PP or TPO will give rise to greatly improved scratch resistance against visibility. The present study also clearly demonstrates the importance and relevance of a model PP system study to reveal conclusive information for establishing structure-property relationship between TPO morphology and its scratch behavior. The implication of the current study signifies that polymer products with improved scratch resistance can be made simply by slight alteration of the processing conditions, whether by post-processing methods (slow cooling/quenching) or by changing the temperature of the mold wall. This fact will surely be attractive to industries where scratch resistance is of utmost importance.

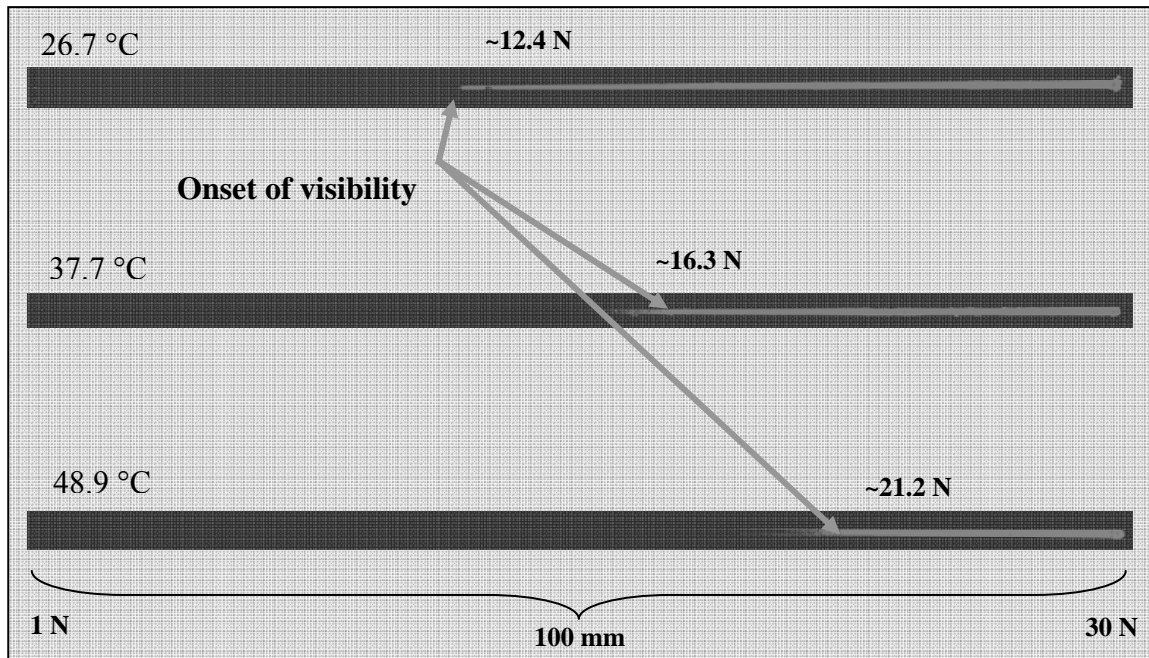


Figure 14 Scanned images of scratched surfaces of an injection-molded TPO specimen subject to different processing conditions.

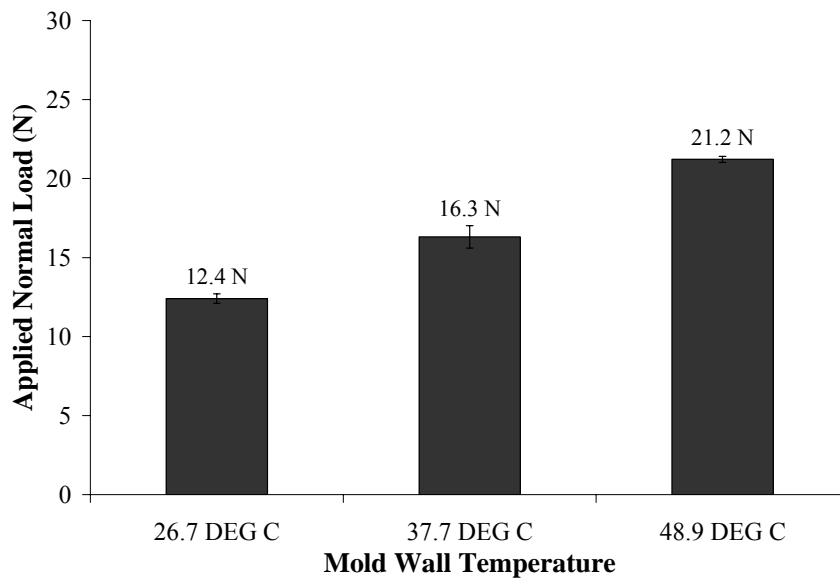


Figure 15 Critical load for the onset of scratch visibility for an injection-molded TPO specimen subject to different processing conditions.

## **CONCLUSION**

Mold temperatures and cooling rates can profoundly affect the mechanical properties of semi-crystalline polymers through the so-called skin-core morphology caused by the heat insulating nature of these materials. In this study, two extreme cooling rates were performed on PP thin sheets to investigate how the processing conditions can affect scratch behavior. The effect of molecular weight has also been investigated and shown to have significant effect on scratch behavior. The resulting critical load for scratch visibility, SCOF, and scratch hardness of the systems were utilized to evaluate scratch performance of PP and TPO. The present study indicates that scratch resistance of both PP and TPOs can be easily improved by controlling their MW and cooling rate during molding.

## **CHAPTER III**

### **SCRATCH BEHAVIOR OF EPOXY BASED NANOCOMPOSITES: EFFECTS OF ADDITIVES OF VARIOUS NATURES**

The effects of nano-additives on the scratch properties of epoxy(DER-332) have been examined. Scratch parameters such as critical load for onset of macro-crack formation, scratch coefficient of friction were utilized in this study while optical and electron microscopy was used to determine failure and fracture patterns caused by the scratch. The findings of this study suggest that the introduction of a nanoparticle or nanoplatelet does not necessarily enhance the scratch resistance of this thermoset polymer. Furthermore, based on the high degree of exfoliation for the nano-additives in the matrix which is evidence of high degrees of nano-dispersion, this factor has actually decreased the materials relative resistance to scratch and therefore in this case the nanocomposites show deteriorated scratch performance compared to the neat system.

#### **INTRODUCTION**

In the past few decades, due to the recognition of the significance and importance of faces, surfaces, and interfacial boundaries, the study of surfaces and interfaces has drawn significant amounts of attention from industrial and academic viewpoints which can accommodating for various applications and purposes such as friction reduction, microscopy techniques, and etc.[45-47]. Tribology, the science and technology of friction,

lubrication, and wear was developed in the 1960s, and with aesthetic and appearance gaining more emphasis from a consumer standpoint, various industries have gained more interest on the issue of developing a test methodology to evaluate tribological properties and finally use this method to determine how various materials will perform in different applications, and better select the material of choice based on a combination of properties, durability, price, availability, aesthetics, and etc.[48].

One of the most essential tribological areas of interest for study and research in the past years has been the scratch deformation and process. The scratch resistance of a material had previously been defined as the ability of the material to withstand abrasion with another body [16,17]. Scratch behaviors of metallic and ceramic materials have been widely explored since the 1950's [6,7]. However, fundamental scratch behavior of polymeric materials has not been the focus of significant research until about a few years ago [8-15]. Previously, attempts to systematically quantify the scratch resistance of polymers have been problematic due to the lack of a general test standard and a set of appropriate evaluation tools. Most recently, Sue et al. have developed a new standard test methodology, ASTM D7027-05, for evaluating scratch resistance of polymers and coatings [18,19]. The standard methodology consists of a linear load increase test and a set of well-defined scratch evaluation parameters, such as scratch visibility, depth, width, and coefficient of friction. Using this methodology, consistent and highly repeatable results have been attained which has been shown in previous studies [4,8,10-14]

Through the detailed examination of the scratch behavior of various polymers, it has been shown that the scratch behavior and response of polymers depends on numerous

parameters [18], such as scratch loading and speeds [20-22], coefficients of friction [8,20-22], geometry and number of scratch tips utilized [8,20-22], and types and amounts of fillers and additives incorporated [20-22]. In addition, material properties will also definitely have an impact on the scratch behavior of plastics. In our previous studies, rudimentary investigations and discussions have been made on how elastic modulus, yield stress, tensile strength, coefficients of friction, and viscoelastic recovery affect scratch behavior of polymers [8, 13, 25]. In order to make an effort to correlate these factors to the scratch behavior of a polymer in a fundamental way, more systematic experimental studies and thorough investigations are still needed.

Recently, material science and engineering has evolved in such a fashion to result in the introduction of multi-phased materials which can even be mixed on a minimal length scale (nano-), which is even comparable to the size of the molecules. These nano-dispersed and nano-mixed materials are the so called newly borne “nanocomposites”, which have been an area of significant industrial and academic interest in the recent years. However, fundamental structure-property relationships in a large portion of polymer nanocomposites are still lacking [49]. The effectiveness of nanofillers on improving physical and mechanical properties of polymer nanocomposites strongly depends on a number of factors including size, shape, aspect ratio, strength, loading level, degree of exfoliation, and their interfacial adhesion in the polymer matrix [50].

Ever since the successful development of nylon/clay nanocomposites that showed great improvements in physical and mechanical properties with only a small amount of clay introduced into the polymer matrix [51-53] in the late 1980s, the pursuits for high

performance polymer nanocomposites have swamped both the scientific community and the industry in the past two decades. Numerous research efforts in this field have been focused on the incorporation of nanoplatelet fillers to greatly enhance their physical, mechanical, and chemical properties in various polymer matrices, including epoxy [54, 55], polypropylene [56-58], polyethylene [59], polyimide [60,61], polystyrene [62-64], poly(methyl methacrylate) [65], etc. Most results have revealed great improvements of polymer properties by a small addition of nanoplatelets (<5 wt%). Important factors that can affect the physical and mechanical properties of nanoplatelet-reinforced polymer nanocomposites include nanoplatelets type [66-70], intercalating agents [71-74], filler loading levels [75-77], and processing [78,79]. In particular, significant efforts have emphasized on achieving maximum level of exfoliation of nanoplatelets in polymer matrices. BP Polymer nanocomposites containing well-dispersed inorganic nanoplatelets, which have at least one dimension in the nanometer range, have been extensively studied [51-61]. To find out how the nanoplatelet dispersion and various other factors influence the properties of polymer nanocomposites, significant research efforts have been carried out in recent years [74-79].

However, due to the fact that both scratch behavior and nanocomposite studies are both relatively new areas of research and therefore have not yet been thoroughly investigated, scratch performance studies of polymer nanocomposites are a field of research that require great amounts of attention in order to relieve any ambiguities.

Therefore the need to further investigate how the introduction of nanoparticles can affect the materials response to a complex stress field such as a scratch deformation, can



be fully sensed. In this study, investigations were based upon three previously analyzed epoxy systems that have been discussed in other previous studies [50, 80, 81].

## **EXPERIMENTAL**

### *Materials*

Flat panels of neat epoxy and CSR or  $\alpha$ -ZrP nanocomposites epoxy were prepared via mold casting. The composition of each system is shown in Table 3.

Preformed CSR particles were used in this study as received from Kaneka Corporation. The diameter for the butadiene rubber core of these CSR particles falls in the 80-90 nm size range, while being covered by a styrene/methyl methacrylate/ acrylonitrile/ glycidylmethacrylate shell acting as a compatibilizer layer which is approximately 10-20 nm in thickness [82, 83].

Table 3 Composition of epoxy systems

System	*Materials	% nano-additive
EP	**DER 332 (neat)	None
ZP	DER 332 + $\alpha$ -ZrP	2 vol%
CSR	DER 332 + CSR	3 wt%

\* All materials were cured via DDS (4,4'-diamino-diphenyl sulfone)

\*\* D.E.R.<sup>TM</sup>332, diglycidyl ether of bisphenol-A (DGEBA)

The  $\alpha$ -ZrP was synthesized by refluxing zirconyl chloride octahydrate ( $\text{ZrOCl}_2 \cdot 8\text{H}_2\text{O}$ , 98%, Aldrich) in 3 M phosphoric acid for 24 hrs. Detailed chemistry and procedures for the synthesis of  $\alpha$ -ZrP can be found elsewhere [84]. A commercial monoamine, polyoxyalkyleneamine (Jeffamine<sup>®</sup> M600, Huntsman Chemical), was used as an intercalating agent for  $\alpha$ -ZrP. The epoxy matrix is composed of diglycidyl ether of bisphenol-A (DGEBA) epoxy resin (D.E.R.<sup>TM</sup> 332 epoxy resin, The Dow Chemical Company), with an epoxy equivalent weight of 171-175 g/mol, and the curing agent, 4,4'-diamino-diphenyl sulfone (DDS, Aldrich).

All the chemicals, except the epoxy resin which was dried in a vacuum oven for 24 hrs prior to curing, were used as received.

### *Heat Treatment (Drying)*

In order to minimize moisture effects, all panels were dried in a Napco E5851 vacuum oven at 70°C for 8 hrs post-curing. Afterwards the samples were kept in a dessicator and exposed to standard relative humidity and temperature conditions 24 hrs prior to testing.

### *Scratch Testing*

A recently developed standardized test method, ASTM D7027-05, was used for the scratch testing of the samples. A constant scratch speed of 10 mm/s with a load range of 1-90 N was used for a scratch length of 100mm to enhance resolution for observing the critical loads for onset of macro-crack formation. The tests were performed at room temperature using a stainless steel spherical shaped scratch tip with 1 mm in diameter. The scratch directions for the testing were all oriented in the same direction to prevent variation in scratch damage due to possible anisotropies. A minimum of 5 tests were performed per sample.

### *Scratch Damage Quantification*

After the scratch tests were performed, the samples were examined using an BX60 optical microscope under bright field conditions in order to determine the onset of macro-crack formation. After measuring the distance of this onset point (x) from the initial point, the critical load for scratch visibility can be calculated by a simple interpolation of the two end loads:

$$F_C = x/L(F_e - F_i) + F_i \quad (1)$$

where  $F_C$ ,  $F_i$ ,  $F_e$ , and  $L$  are the critical load, initial load, end load, and scratch length, respectively.

#### *Scratch Coefficient of Friction*

The scratch coefficient of friction (SCOF) is defined as the ratio of the tangential force to the normal force at each loading point. The scratch testing instrument utilized in this study is capable of *in-situ* determining the actual normal and tangential force at each point of the scratch which results in SCOF:

$$SCOF = \frac{F_z}{F_x} \quad (2)$$

#### *Optical Microscopy Observation of Scratch Damage*

In order to observe the differences in the scratch damage of the different systems and better evaluate the materials response to the scratch OM and SEM was performed. Top view OM and SEM images of the scratch path were taken to determine the macro-crack formation and mar transitions. Longitudinal sections of the scratch groove along the scratch direction were examined to determine and compare the subsurface damage caused by the scratch process. The OM images were captured using an Olympus BX60 optical microscope under cross-polarized as well as bright field conditions. Scanning Electron Microscopy was performed on a JEOL-JSM 6400 system, operated at 15 kV.

### *Surface Roughness Measurements (Profilometry)*

In order to investigate surface roughness along the scratch path at the mar transition, a Dektak 3 Stylus Profilometer (Veeco Metrology, Inc.) was utilized to measure the vertical profiles of the scratch in all three samples. The radius of the diamond conical stylus used was 12.5  $\mu\text{m}$  and the normal force applied to the stylus was the factory-set value of 50 milligrams. The analog signal generated from the vertical fluctuations of the diamond stylus is converted into a digital signal which ranges in height from 10 to 65,000 nm. The horizontal resolution is controlled by the scan speed and scan length used during measurements.

## **RESULTS AND DISCUSSION**

It has previously been shown that when scratch testing brittle or semi-brittle polymeric materials, in an attempt to quantify the materials resistance to scratch deformation, the onset of crack formation is of significant importance. This fact is mainly due to the drastic alteration of surface roughness and initiation of material discontinuity at this transition which both contribute to light scattering effects causing this transition to be observed as the onset of scratch visibility. The onset of macro-crack formation and the corresponding normal loads at this point in the two nanocomposite systems (ZRP and CSR) has been shown in Figure 16, while the neat system did not show any signs of macro-crack formation up to a normal load equivalent to 90N. A qualitative comparison of the average values of these critical loads can be seen in Figure 17. It can be observed that

the addition of these nanoparticles leads to a reduction in the critical normal load at this transition, independent of the additive's nature.

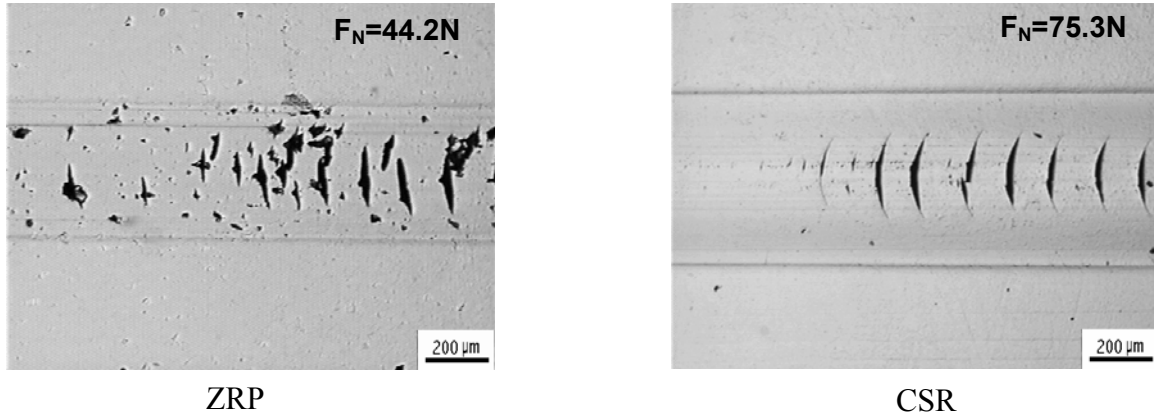


Figure 16 Optical micrographs of onset of macro-crack formation

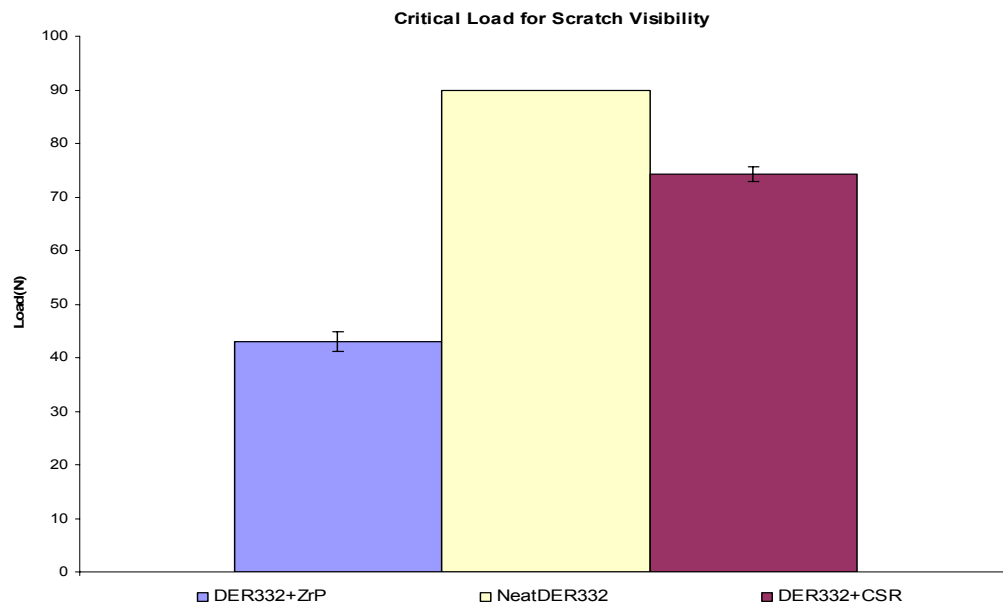


Figure 17 Critical normal load values for onset of damage

The SCOF curves of the three systems are shown as a function of distance from the start point of the scratch in Figure 18. It can be seen that the SCOF of ZRP is noticeably higher than CSR and NE which is an indicator of higher tangential loads caused by the scratch tip during the scratch process due to frictional forces which itself can facilitate the formation of macro-cracks. In Figure 19, tangential loads of the systems are shown as a function of the distance along the scratch. This also emphasizes on the higher tangential load for ZRP at the same normal loads while indicating lower observed tangential loads for NE compared to CSR at normal loads higher than 50N. Due to the fracture mechanisms observed in brittle and semi-brittle materials subjected to scratch conditions [Xiang], the shear force is of significant importance in the formation of macro-cracks.

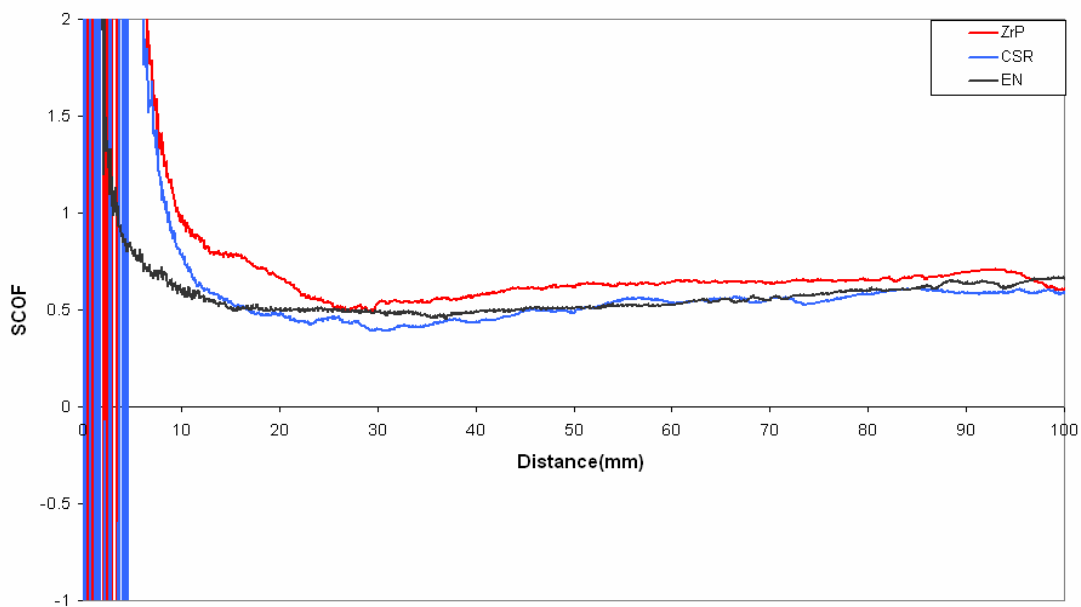


Figure 18 SCOF comparison of three systems

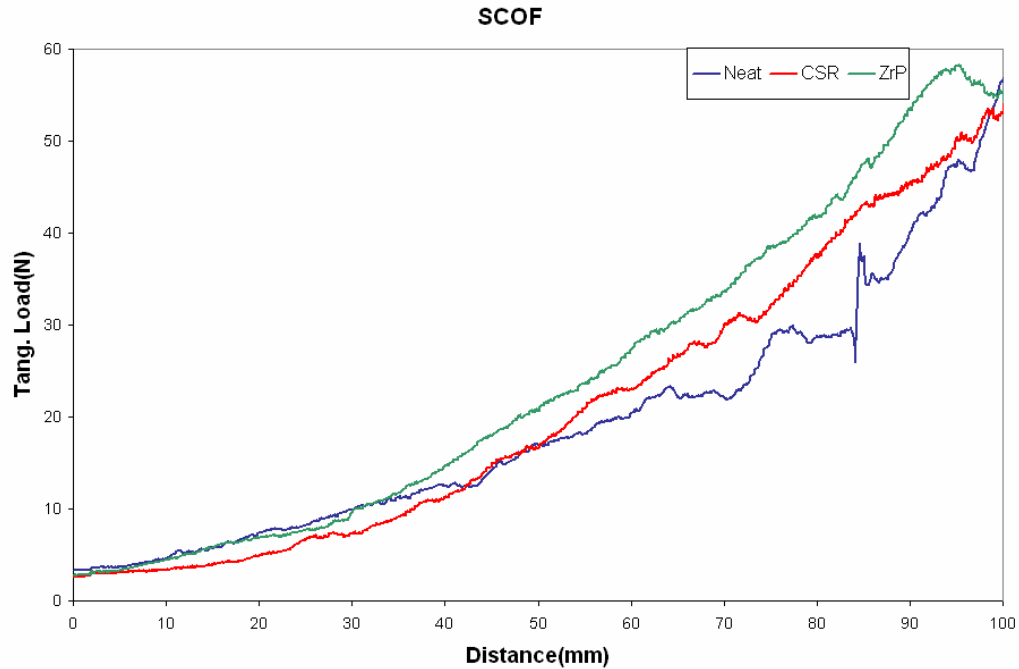


Figure 19 Tangential load values along the scratch path

Optical micrographs of the scratch valley's longitudinal sections along the scratch path for CSR and ZRP systems at the macro-crack formation transition under cross polarized light have been shown in Figure 20. The comparison of the bright appearing zones characterized by the birefringence caused by relative orientations due to plastic deformation suggest that ZRP and CSR both undergo subsurface plastic deformation, while only the CSR system experiences considerable amounts of plastic deformation in parts of the scratch groove located above the center line of the valley which all macro-cracks are initiated from. It can be observed that the depth of the subsurface plastic zone for CSR is slightly larger than that of ZRP, while based on relative normal loads and



modulus comparisons of the two systems higher variations are expected. This matter can be explained by the stress state which these materials are subjected to during the scratch process. The stress state beneath the scratch surface will be highly dependent on a *combination of shear and compressive stresses with minimal tensile effects, while the shear stress induced on the subsurface will lose significance at higher depths in this region*. Furthermore, after the transition point the frequency of macro-crack occurrence in ZRP is observed to be higher than CSR, which can be attributed to the fact that this system shows more brittle characteristics and lower fracture toughness which is listed in Table 4. Furthermore, the large plastic deformation in the scratch valley for the CSR system can be related to the more ductile nature of this system and the higher corresponding normal loads induced at this transition.

Table 4 Glass transition temperature and mechanical properties of systems

	Neat Epoxy	Epoxy/CSR	Epoxy/ $\alpha$ -ZrP
Tensile Modulus (GPa)	$2.90 \pm 0.05$	$2.56 \pm 0.06$	$3.72 \pm 0.21$
KIc (MPa*m <sup>1/2</sup> )	$0.72 \pm 0.02$	$0.92 \pm 0.08$	$0.79 \pm 0.04$
Elongation at break (%)	$4.1 \pm 0.4$	$6.5 \pm 0.5$	$3.9 \pm 0.3$
Tg (°C)	215	129	150

Optical micrographs of the scratch area subsequent to the macro-crack formation transition for CSR and ZrP have been shown in Figure 21. It can be observed that besides the main bow shaped macro-cracks that have previously been discussed, secondary cracks parallel to the scratch direction have been formed which appear to be at higher depths compared to the original ones, penetrating into the subsurface region. These secondary cracks are an indicator of the complexities in the stress field generated during the scratch process causing multiple fracture mechanisms.

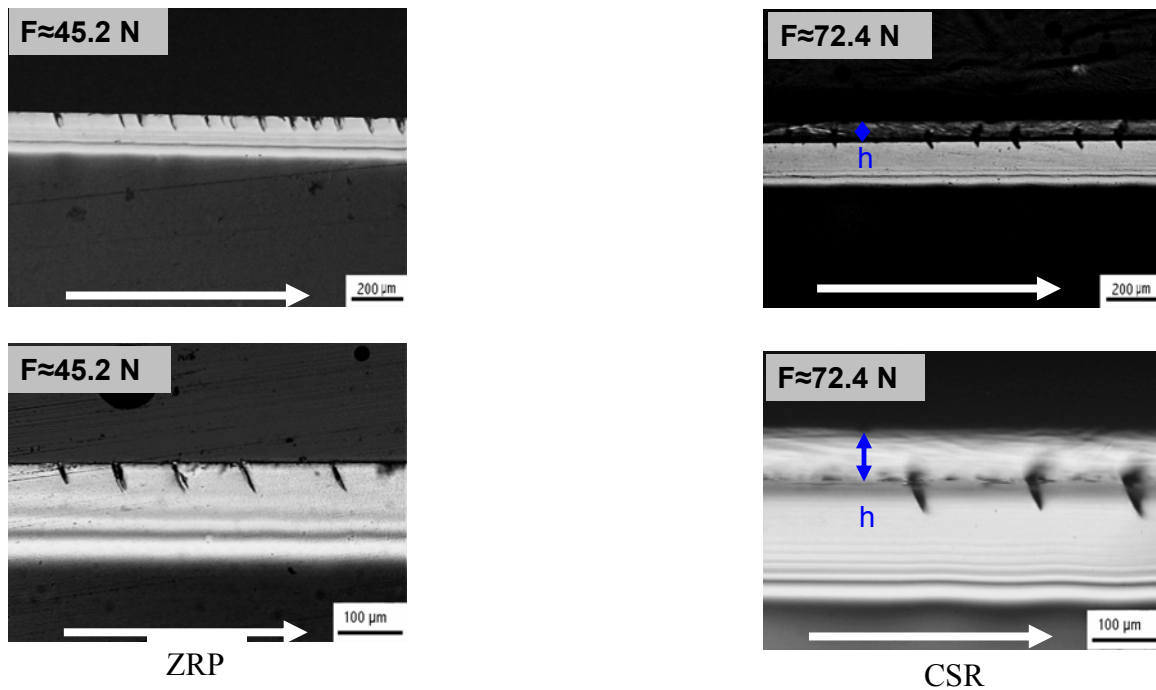


Figure 20 Longitudinal cross-sections of scratch valley at the onset for macro-crack formation

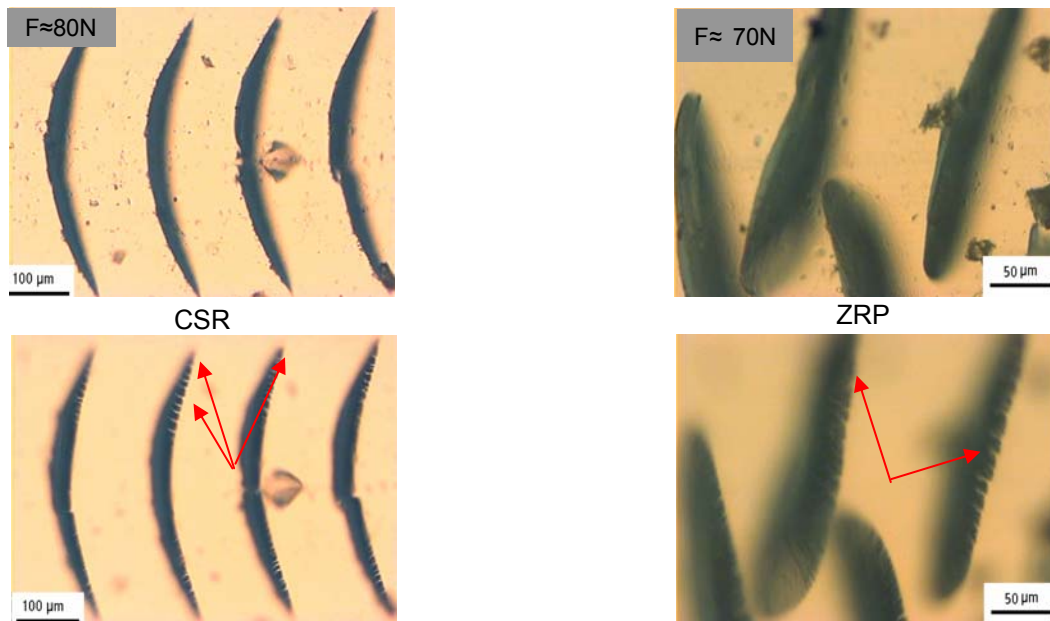


Figure 21 Evidence of secondary crack formation shown by optical microscopy

In Figures 22 and 23, SEM micrographs of the ZRP and CSR scratch zones at the noted corresponding loads have been shown. Comparison of the images shown in 7a and 8a indicate that the surface crack occurrence density is higher in ZRP, which itself is a support to the previously mentioned fact, regarding the subsurface region initiating from the more brittle nature of ZRP. Furthermore, comparing Figures 22b and 23b, it is noticed that at higher magnifications the brittle natured fracture for ZRP is completely evident at this scale characterized by the shattering-like effect with sharp boundaries while the fracture induced on CSR shows some plastic tearing-like features with areas of the scratch which appear to have experienced relatively large plastic deformation before fracture.

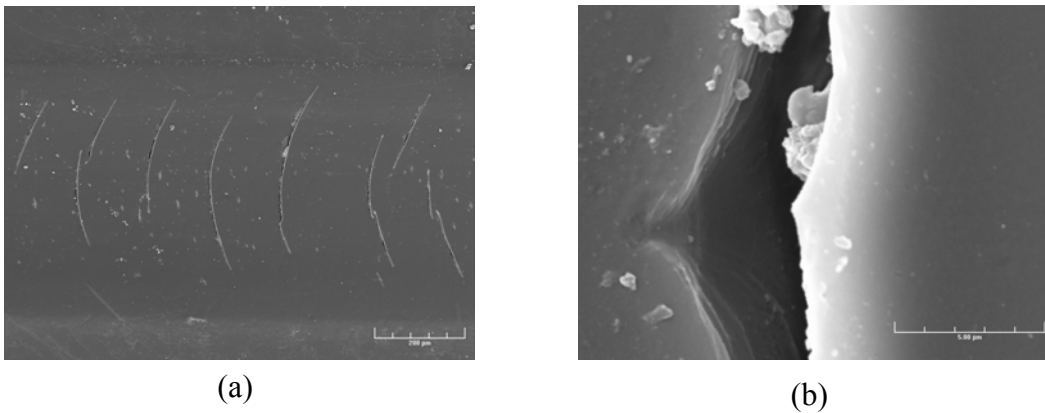


Figure 22 SEM images of CSR

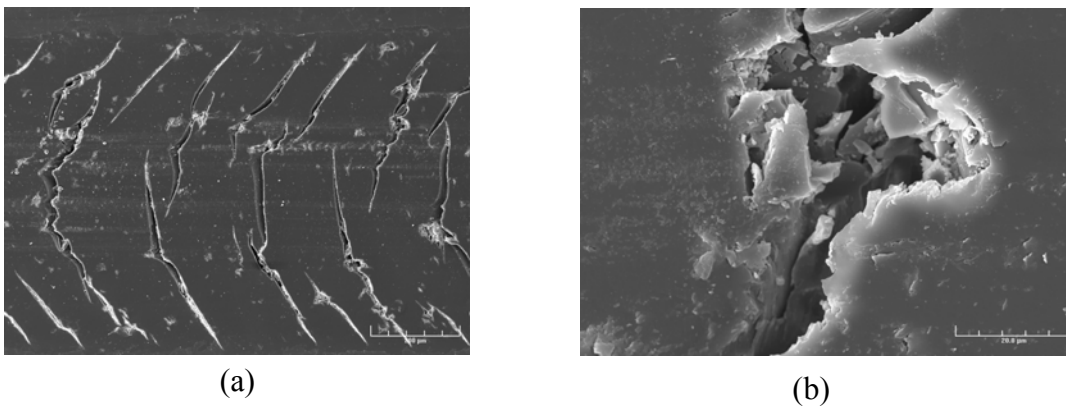


Figure 23 SEM images of ZRP

Another area of interest created during the scratch process is the mar damage and the related transition. This transition is characterized by the variation of the material's gloss, which can also be detected visually due to variation in the materials surface

roughness at this point. From a mechanical point of view, in this case mar can be recognized as the region from which the scratch tip interacts with the material to flatten the mar area and have a so called ironing effect due to plastic and permanent deformation caused in the material, while regions prior to this only undergo linear and non-linear elastic deformations which appear to be fully recovered after the removal of the stress. Figure 24 illustrates optical micrographs of the mar transition where the corresponding normal loads for the systems have been noted. SEM micrographs of this transition have been shown in Figure 25 for further assessment.

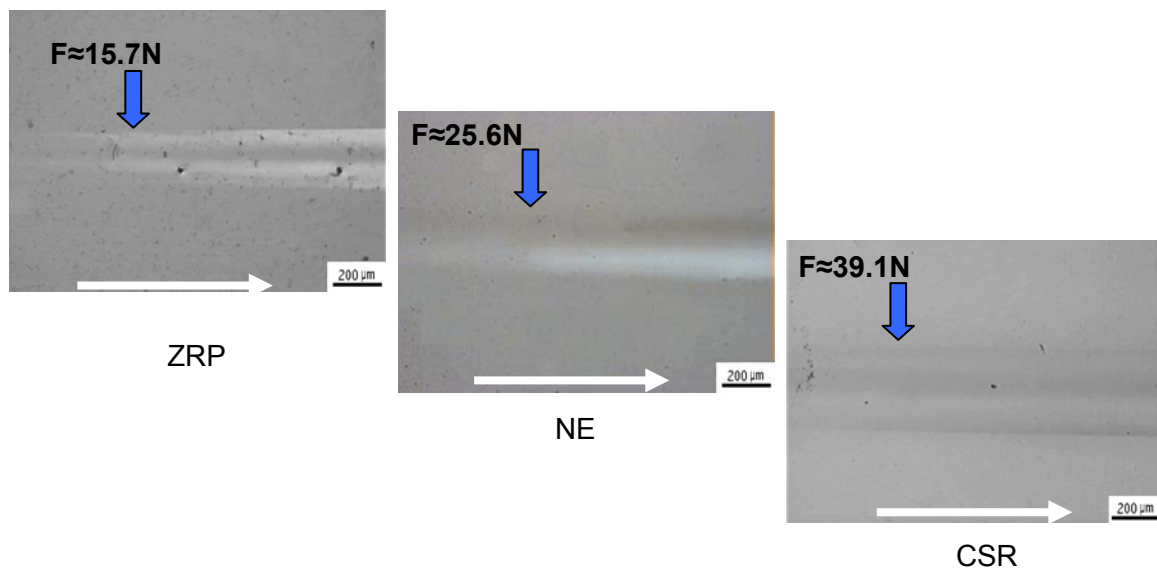


Figure 24 Optical micrographs of mar transition

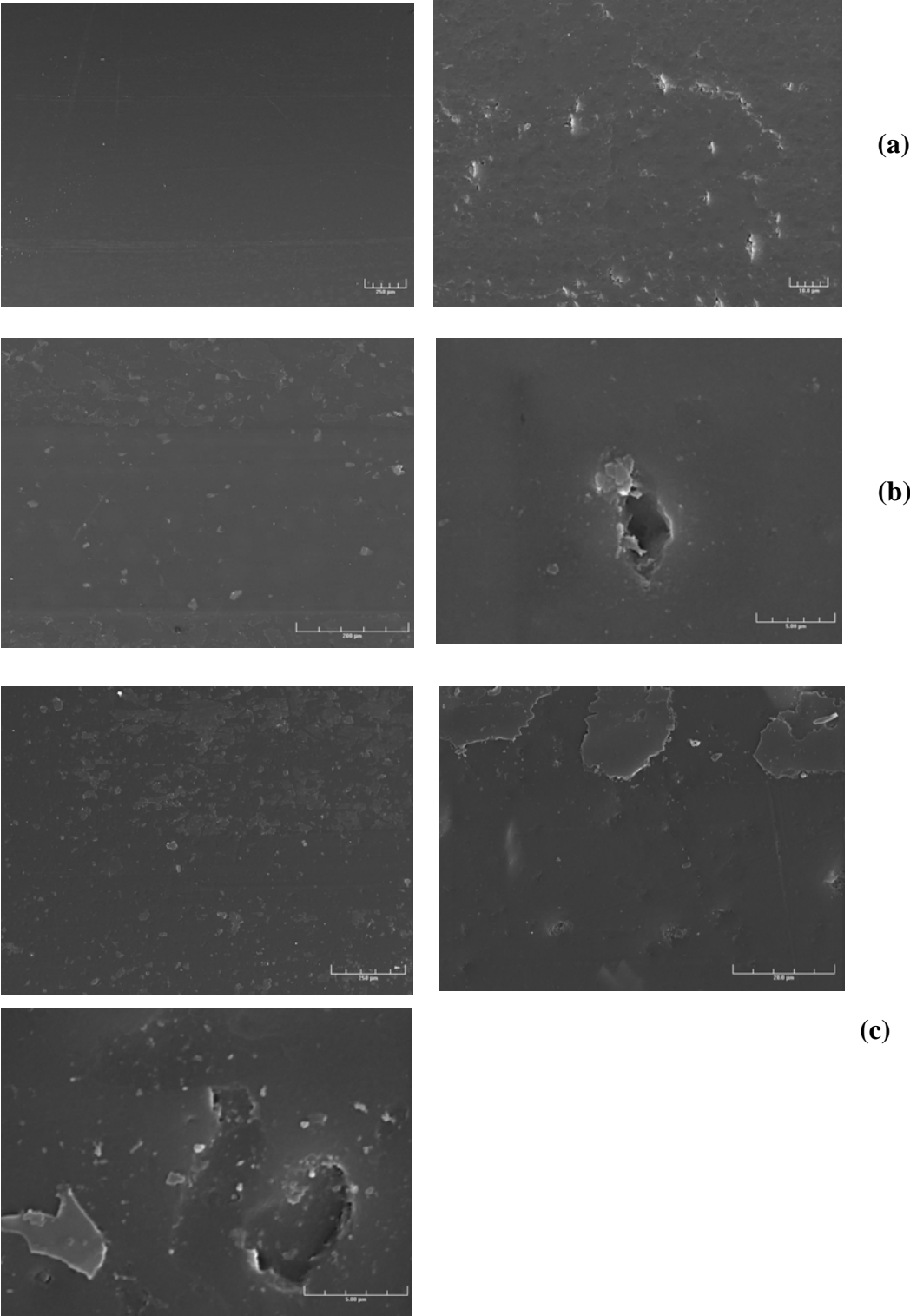


Figure 25 SEM images of various observations in mar region

In order to further evaluate the mar transition in the three systems, surface roughness profiles from cross sections of the scratch perpendicular to the scratch direction, before and after this transition have been shown in Figure 26. It can be noticed that in all three cases, the relative surface roughness characterized by the density of peaks observed decreases after the mar transition. Attention can be drawn to Figure 27 which illustrates the longitudinal surface roughness profiles along the scratch path before and after the mar transition for the ZRP and CSR systems. The decrease in surface roughness after the mar transition can be noticed in this case as well.

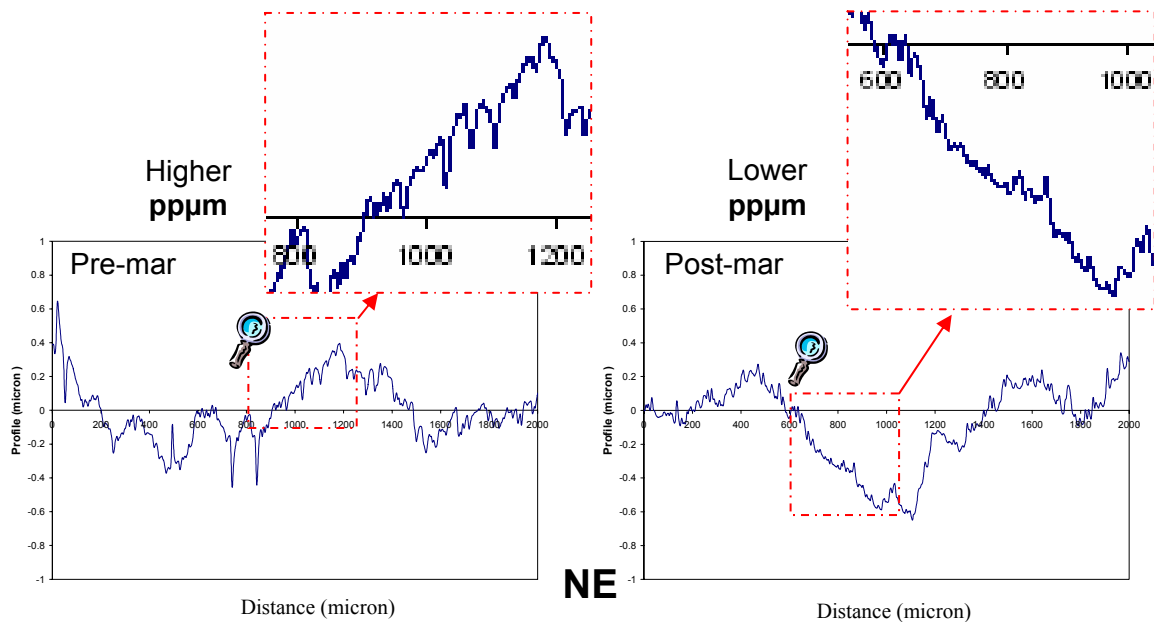


Figure 26(a) Surface roughness profiles before and after mar transition for NE

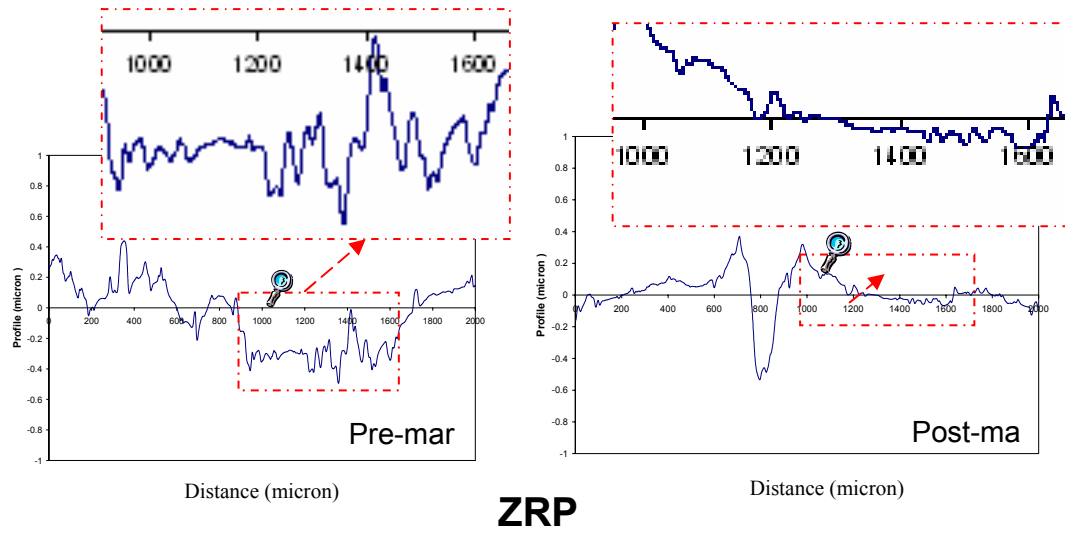


Figure 26 continued (b) Surface roughness profiles before and after mar transition for ZRP

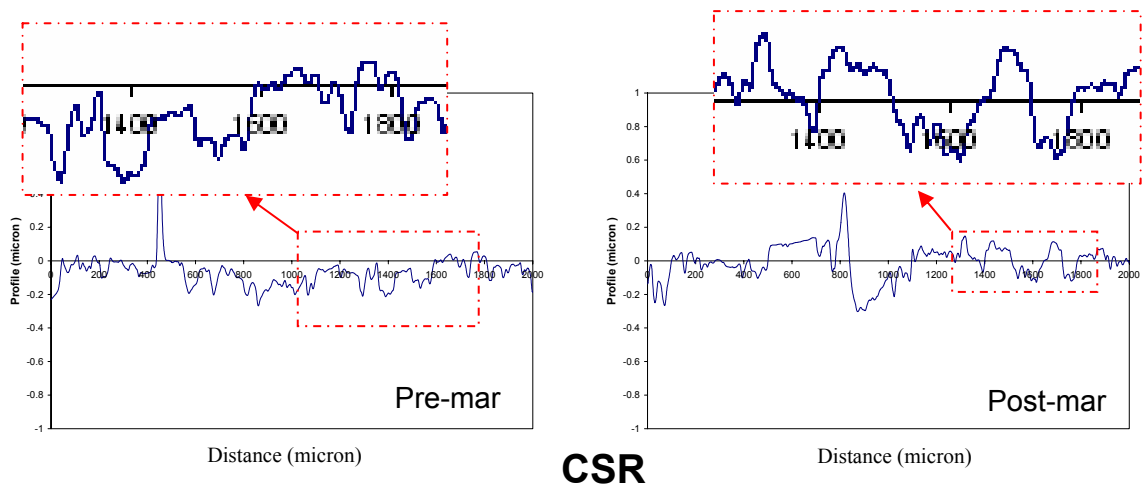


Figure 26 continued (c) Surface roughness profiles before and after mar transition for CSR



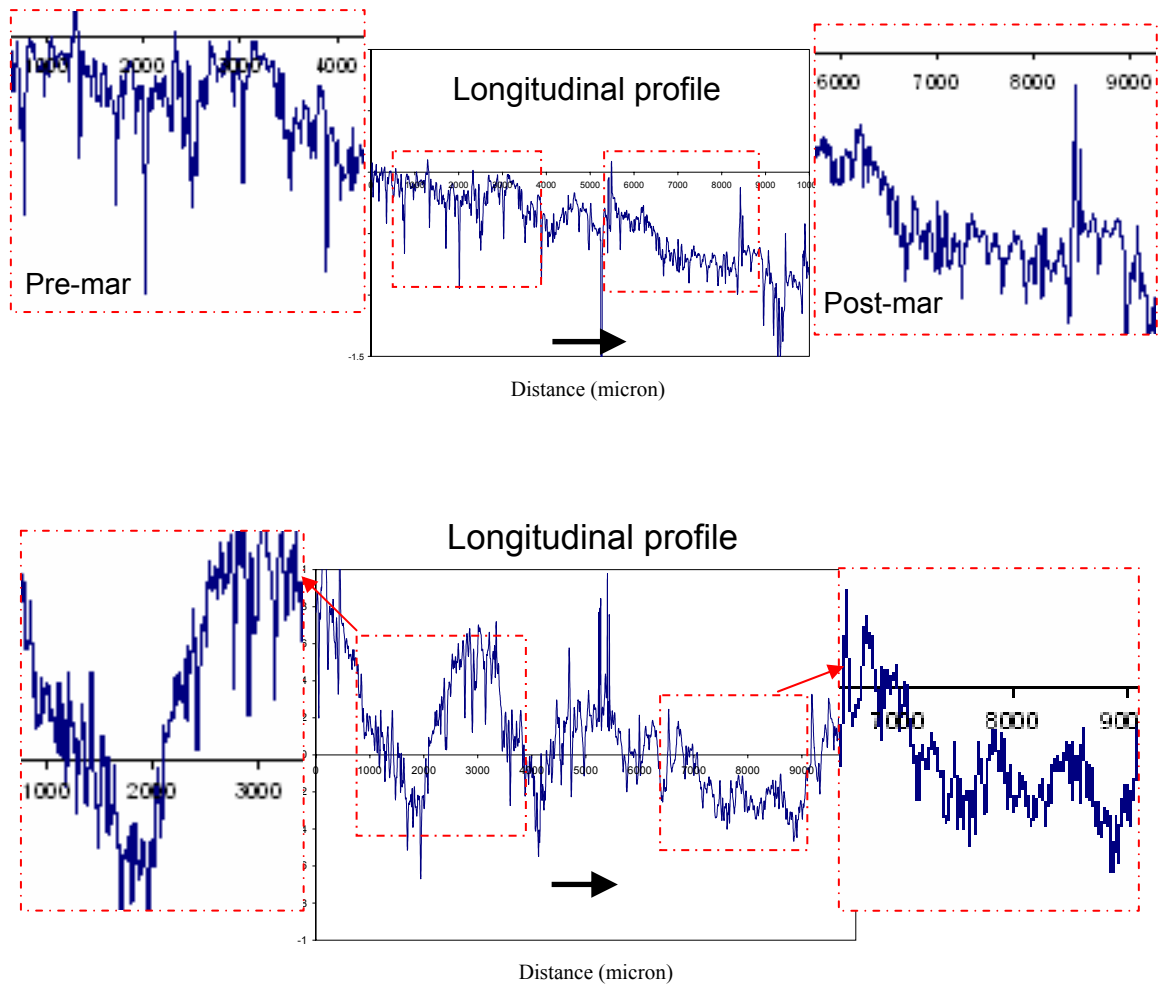


Figure 27 Surface roughness profiles in the longitudinal direction for (a) CSR and (b) ZRP

## CONCLUSION

The addition of nano-sized particles can contribute to enhanced mechanical properties such as elastic modulus or elongation at break which is measured based upon simplistic induced stress fields. However, when these materials are subjected to stress fields generated by a scratch tip, it has been observed that critical loads for crack

formation and hence scratch visibility decreases. Therefore the observed resistance to scratch deformation for the mentioned multi-phased material decreases compared to a neat system of the same material.

Furthermore, in this study various crack formations prior to the macro-crack formation transition were observed and a certain emphasis can be put on the importance of compatibility between the scratch deformation length-scale and the scale which is used to investigate the effects of this deformation and fracture mechanisms.

## **CHAPTER IV**

### **CONCLUSIONS AND REMARKS**

This current research effort was intended to achieve better understanding on the complex relationship between various material properties (e.g. physical, mechanical, thermo-mechanical, etc.) and the behavior which the material demonstrates during a scratch process. In order to examine both ductile and brittle cases and compare the responses and failure mechanisms which each of these material categories exhibit, two different studies on PP and epoxy were performed. During the evaluation of various scratch parameters for the studied systems, based on the validity of each parameter to confirm the cause of the scratch deformation and the capability to explain the differences in the scratch patterns it can be concluded that some parameters may lose significance in certain applications e.g. scratch hardness was shown to be nearly constant in all cases of the PP study.

Based on the PP study the effects of material properties and structural morphology on the scratch behavior of these materials have been explained. The results of the epoxy nanocomposite study illustrates the possible and mainly unknown short-comings that fully exfoliated nanocomposites can show when subjected to complex mechanisms such as the induced stress field related to a scratch deformation. Although fully exfoliated nanocomposites are known to display significantly enhanced performance in some aspects, these multi-phased materials may also exhibit some inferior qualities and properties especially under exposed complexities.

Furthermore, based on the comparison of fracture and failure mechanisms observed in the PP and epoxy studies, conclusions are made based upon scratch patterns formed in the materials surface and its' correlation with the ductile or brittle nature of the material.

Finally, suggestions are given for further studies attempting to fully understand scratch behavior of polymers and predict the scratch resistance of polymers simply based upon its' material properties. Although recently a great deal of attention has been drawn to scratch research, in order to gain fundamental knowledge on a material's response to scratch and correlate this to a set of defined material properties significant experimental and analytical efforts are needed in future works.

## **CONCLUSIONS ON PP STUDY**

Ductile and semi-ductile materials such as PP exhibit formation of a fish scale type pattern above certain normal loads applied in the scratch process which is known to result in scratch visibility. This fish scale pattern is formed due to the ductile nature of the material deformed by the scratch tip resulting in permanent plastic deformations. Increases in molecular weight of thermoplastic polymers are known to enhance some mechanical properties which as discussed in Chapter II lead to improved scratch performance. Another factor that can have a major influence on the material properties of semi-crystalline polymers such as PP is the degree of crystallinity. Based on the findings of this study it was shown that crystallinity increases can also result in enhanced scratch resistance which can mainly be attributed to the decrease in frictional forces resulting in

lower observed SCOF and therefore tangential forces.

## **CONCLUSIONS ON EPOXY STUDY**

Dispersion of two components of a composite material is normally sought to the highest extent due to the increasing interfacial area between the two phases which can enhance desired properties. However, full dispersion of the separate phases of polymeric materials has always been challenging. Even more challenging is acquiring high degrees of exfoliation for polymer nanocomposites which is known to dramatically improve some of their properties. However, in this study it was shown that fully exfoliated nanocomposites do not necessarily exhibit improved scratch resistance compared to the neat system, regardless of the nano-additives nature (brittle or ductile).

The exhibited failure and fracture patterns in the epoxy based systems during the scratch process indicate high levels of complexity in the scratch stress field causing various toughening and failure mechanisms to coincide that have been explained in Chapter III. However, the main observed fracture pattern is the bow shaped macro-cracks which are formed due to the combined compressive and shear stress which has been explained elsewhere [12].

Based on the findings of this study, the mar region can be described as a relative decrease in surface roughness which occurs when the scratch stress field surpasses the requirements of the material to exhibit non-linear elastic behavior or to locally deform. This decrease in surface roughness is the main cause for the alteration of material gloss at the mar transition. Furthermore, evaluation of the mar region at higher magnifications

uncovers micro-crack formation in this region. Therefore, the length-scale which mar and scratch evaluations are based upon can be misleading and the utilized evaluation length scale should be in the same range as the type of scratch deformation whether macro, micro, or nano-scale.

### **CONCLUSIONS ON FAILURE AND MATERIAL NATURE**

The observed failure mechanisms which polymeric materials exhibit when subjected to scratch can depend on various factors. One of the most important of these factors is the physical and mechanical nature of the material, which itself can determine whether the surface damage will exhibit cracking, material removal, tearing, ductile drawing or etc. or even a combination of more than one feature. Therefore, when examining polymeric systems which do not exactly fall into either categories of ductile or brittle at testing temperatures, caution should be carried out especially while examining the damage type and extent and scale of occurrence.

### **CONCLUSIONS ON EFFECTIVE PARAMETERS**

Although scratch hardness was previously considered as one of the most reliable and differentiating scratch evaluation parameters in scratch research, this parameter has shown to be incapable of differentiating between systems which show similar mechanical behavior. However, SCOF and critical loads for onset of mar and visibility have been shown to be effective in all encountered cases while scratch hardness is not recommended in order to evaluate systems within the same range of mechanical properties

## **RECOMMENDATIONS FOR FUTURE WORK**

Based on previous and current studies and their findings, in order to fully understand the scratch behavior of a polymer and possibly introduce material scratch properties which can effectively predict the behavior and response of the polymer under scratching conditions, significant efforts are still needed in this area. On the other hand, based on the findings of macro-scratch evaluations, examination of micro and nano-scaled scratch followed by the comparison of scratch behavior and damage on three various scales fundamental conclusions can be made.

## REFERENCES

- [1] ASTM International, "ASTM G 171-03: Standard test method for scratch hardness of materials Using a Diamond Stylus," *Annual Book of ASTM Standards*, 3-02, 2003.
- [2] International Organization for Standardization, "ISO 12137-1:1997 – Determination of mar resistance – Part 1: Method using a curved stylus," *ISO Standards*, 87.040, 1997.
- [3] International Organization for Standardization, "ISO 12137-2:1997 – Determination of mar resistance – Part 2: Method using a pointed stylus," *ISO Standards*, 87.040, 1997.
- [4] Lim, G.T., Wong, M., Reddy, J.N., and Sue, H.-J., 2005 "An integrated approach towards the study of scratch damage of polymer," *J. Coating Technol. Res.*, **2**(5), 361-369.
- [5] Bowden, F.P. and Tabor, D. *The Friction and Lubrication of Solids*, Clarendon Press, Oxford, 1954.
- [6] Bowden, F.P. and Tabor, D., in "*The Friction and Lubrication of Solids*" Part I (Oxford University Press, Oxford, 1950) p.33.
- [7] Bowden, F.P. and Tabor, D., in "*The Friction and Lubrication of Solids*" Part II (Oxford University Press, Oxford, 1964) p.350.
- [8] Xiang, C., Sue, H.-J., Chu, J, and. Coleman, B., 2001, *J. Polym. Sci. Polym. Phys.* **39**, 47–59.
- [9] M. Sato and O. Ishizuka, *Kobunshi Kagaku*, 1966, **23**, p.800.
- [10] M. Wong, A. Moyse, F. Lee, and H.-J. Sue, 2004, *J. Mater. Sci.*, **39**, p.3293.
- [11] M. Wong, G.T. Lim, A. Moyse, J.N. Reddy, and H.-J. Sue, *Wear*, 256, 1214 (2004).
- [12] C. Xiang, H.-J. Sue, J. Chu, and B. Coleman, *J. Polym. Sci. Part B: Polym. Phys.*, 39, 47 (2001).



- [13] H. Jiang, G.T. Lim, J.D. Whitcomb, and H.-J. Sue, "FEM Parametric Study on Scratch Behavior of Polymers", *J. Polym. Sci.-Polym. Phys. Ed.*, in press.
- [14] R. Browning, G. Lim, A. Moyse, L. Sun, H.-J. Sue, "Effects of Slip Agent and Talc Surface Treatment on the Scratch Behavior of TPOs", *Polym. Eng. Sci.*, **46**, 601-608(2006).
- [15] J.S.S. Wong, H.-J. Sue, K.-Y. Zeng, R.K.Y. LI, and Y.-W. Mai, "Surface Damage of Polymers in Nanoscale", *Acta Mater.*, **52**, 431-443(2004).
- [16] Wu, S., Sehanobish K., Christenson C., Newton J., *Proceedings of ACS Polymeric Materials Science and Engineering*, vol. 79 (1998), p. 343.
- [17] Sadati M., Mohammadi, N., Qazvini N.T., Tahmasebi, N., Koopahi, S, *Progress in Organic Coatings*, v 53, n 1, 2005, p 23-28.
- [18] Wong, M., Lim, G.T., Moyse, A., Reddy, J.N., Sue, H.J., *Wear*, 256(2004), p.1214-1227.
- [19] Wong, M., Moyse, A., Lee, F., Sue, H.-J., *J. Materials Science* 39 (2004), 3293-3308.
- [20] Briscoe, B.J., Evans, P.D. Pelillo, E. and Sinha, S.K., *Wear* 200 (1996), pp. 137-147
- [21] Fujiyama, M. In Polypropylene, structure and morphology; Karger-Kocsis, J., Ed.; Chapman & Hall: London, 1995; pp. 167-204.
- [22] Kalay, G.; Bevis, M. J. In Polypropylene, an A-Z Reference; Karger-Kocsis, J., Ed.; Kluwer Publishers: Dordrecht, 1999; pp. 38-46.
- [23] Karger-Kocsis, J. In Structure Development during Polymer Processing; Cunhaand, A. M.; Fakirov, S., Eds.; Kluwer Academic: Dordrecht, 1999.
- [24] Chu, J., Rumao, L., and Coleman, B., *Polym. Eng. Sci.* 38, 11 (1998), pp. 1906-1914.
- [25] Chu, J., Xiang, C., Sue, H.-J., and Hollis, R.D., *Polym. Eng. Sci.* 40, 4 (2000), pp. 944-955.
- [26] Xu T., Yu J., Zhihao J., *Materials and design*, 22(2001), 27-31.
- [27] Way, J. L.; Atkinson, J. R.; Nutting, J. *J Mater Sci* 1974, 9, 293.

- [28] Maspoch M. Ll., Gamez-Perez J., Giminez E., Santana O., Gordillo A., *J. of Applied Polym. Sci.*, 93(2004), 2866-2878.
- [29] Briscoe, B.J., Pelillo, E., and Sinha, S.K., *Polym. Eng. Sci.* 36 24 (1996), pp. 2996–3005.
- [30] Briscoe, B.J., Evans, P.D., Biswas, S.K., and Sinha, S.K., *Tribol. Int.* 29 2 (1996), pp. 93–104.
- [31] Kody, R.S., and Martin, D.C., *Polym. Eng. Sci.* 36 2 (1996), pp. 298–304.
- [32] Alberola, N.; Fugier, M.; Petit, D.; Fillon, B. *J of Material Science* 1995, 30, 1187.
- [33] Poussin, L.; Bertin, Y. A.; Parisot, J.; Brassy, C. *Polymer* 1989, 39, 4261.
- [34] Pick L.T., Harkin-Jones E., Oliveira M.J., Cramez M.C., *J. of Applied Polym. Sci.*, Vol. 101,1963-1971(2006).
- [35] Ismail, Y. S.; Richardson, M. O. W.; Olley, R. H. *J Appl Polym Sci*, 79, 1704( 2001).
- [36] Daniels, C. A. *Polymers: Structure and Properties*; Technomic Publishing Company: Lancaster, PA, 1989.
- [37] De Rosa C., Auriemma F., de Ballesteros O.R., *Macromolecules*, 36, 7607-7617(2003).
- [38] Ogawa T., *J. of Applied Polym. Sci.*, 44, 10, 1869-1871(1992).
- [39] J. R. Martin, J. F. Johnson, and A. R. Cooper, *J. Macromol. Sci. Rev. Macromol. Chem.*, C8,57 (1972).
- [40] P. J. Flory, *J. Am. Chem. SOC.* 6, 7,2048 (1945).
- [41] N. Nakano and S. Hasegawa, *J. SOCM. ater. Sci., Jpn.*, 33,1206 (1984).
- [42] N. Nakano and S. Hasegawa, *J. SOCM. ater. Sci., Jpn.*, 35,1060 (1986).
- [43] Zhu P.W., Edward G., *Macromolecular Materials and Engineering* 288(4), 301-311 (2003).
- [44] Fujiyama M., Masada I., Mitani K., *J. of Applied Polym. Sci.* 78(10), 1751-1762 (2000).

- [45] A. A. Betiana, M. M. Reboredo, N. E. Marcovich, *Composites Part A*; 38, 2007, 1507-1516
- [46] F. Monroy, F. Ortega, R.G. Rubio, and M.G. Velarde, *Advances in Colloid and Interface Science*, 2007 in press
- [47] X. Wang, X. Wang, and Z. Chen, *Polymer* 48, 2007, 522-529
- [48] M. Barletta, L. Lusvardi, F. Pighetti Mantini, G. Rubino, *Coating and Surface Technology*, 201, 2007, 7479-7504
- [49] H. -J. Sue, et. al., *Acta Material*, 52, 2004, 2239-2250
- [50] W. J. Boo et. al., *Polymer* 48, 2007, 1075-1082
- [51] Kojima Y, Usuki A, Kawasumi M, Okada A, Kurauchi T, Kamigaito O. *J Polym Sci Part A Polym Chem* 1993;31:983.
- [52] Kojima Y, Usuki A, Kawasumi M, Okada A, Fukushima Y, Kurauchi T, et al. *J Mater Res* 1993;8:1185.
- [53] Yano K, Usuki A, Okada A, Kurauchi T, Kamigaito O. *J Polym Sci Polym Chem* 1993;31:2493.
- [54] Kinloch AJ, Taylor AC. *J Mater Sci Lett* 2003;22:1439.
- [55] Liu TX, Tjiu WC, Tong YJ, He CB, Goh SS, Chung TS. *J Appl Polym Sci* 2004;94:1236.
- [56] Hasegawa N, Okamoto H, Kato M, Usuki A. *J Appl Polym Sci* 2000;78: 1918.
- [57] Kato M, Usuki A, Okada A. *J Appl Polym Sci* 1997;66:1781.
- [58] Kawasumi M, Hasegawa N, Kato M, Usuki A, Okada A. *Macromolecules* 1997;30:6333.
- [59] Chrissopoulou K, Altintzi I, Anastasiadis SH, Giannelis EP, Pitsikalis M, Hadjichristidis N, et al. *Polymer* 2005;46:12440.
- [60] Lan T, Kaviratna PD, Pinnavaia TJ. *Chem Mater* 1994;6:573.
- [61] Tyan HL, Liu YC, Wei KH. *Chem Mater* 1999;11:1942.

- [62] Hasegawa N, Okamoto H, Kawasumi M, Usuki A. *J Appl Polym Sci* 1999;74:3359.
- [63] Essawy HA, Badran AS, Youssef AM, Abd El Hakim AA. *Macromol Chem Phys* 2004;205:2366.
- [64] Morgan AB, Harris JD. *Polymer* 2004;45:8695.
- [65] Zhu J, Start P, Mauritz KA, Wilkie CA. *Polym Degrad Stab* 2002;77:253.
- [66] Usuki A, Kojima Y, Kawasumi M, Okada A, Kurauchi T, Kamigaito O. *Abstr Pap Am Chem Soc* 1990;200:218.
- [67] Skowronski JM, Shioyama H. *Carbon* 1995;33:1473.
- [68] Shioyama H. *Carbon* 1997;35:1664.
- [69] Harris DJ, Bonagamba TJ, Schmidt-Rohr K. *Macromolecules* 1999;32:6718.
- [70] Kellar JJ, Herpfer MA, Moudgil BM, Society for Mining Metallurgy and Exploration (U.S.). *Functional fillers and nanoscale minerals*. Littleton, Colo: Society for Mining Metallurgy and Exploration; 2003.
- [71] Kim JK, Hu CG, Woo RSC, Sham ML. *Compos Sci Technol* 2005;65:805.
- [72] Wang Z, Pinnavaia TJ. *Chem Mater* 1998;10:1820.
- [73] Hasegawa N, Kawasumi M, Kato M, Usuki A, Okada A. *J Appl Polym Sci* 1998;67:87.
- [74] Liu J, Boo W-J, Clearfield A, Sue H-J. *Mater Manuf Process* 2005;20:143.
- [75] Lan T, Pinnavaia TJ. *Chem Mater* 1994;6:2216.
- [76] Messersmith PB, Giannelis EP. *Chem Mater* 1994;6:1719.
- [77] Giannelis EP. *Adv Mater* 1996;8:29.
- [78] Okamoto M, Morita S, Taguchi H, Kim YH, Kotaka T, Tateyama H. *Polymer* 2000;41:3887.

- [79] Weon JI, Sue HJ. *Polymer* 2005;46:6325.
- [80] H.-J. Sue, E. I. Garcia-Meitin, P. C. Yang, *Composites* 24(6), 1993, 495-500
- [81] W. J. Boo et. al., “Effect of Nanoplatelet Dispersion on Mechanical Behavior of Polymer Nanocomposites”, *J. Appl. Polym. Sci.*, 2007, in press
- [82] H.-J. Sue, E. I. Garcia-Meitin, D.M. Pickelman, *Elastomer technology handbook*, CRC press, 1993, p.662, Chapter 18
- [83] H.-J. Sue, *Polym. Eng. Sci.*, 31, 1991, p. 275
- [84] H.-J. Sue et. al., *Chem Mater*, 16, 2004, p.242

## VITA

Mr. Ehsan Moghbelli studied in USA for elementary and middle school while finishing high school in Iran. Mr. Moghbelli earned his Bachelor of Science in Polymer Engineering in 2004 at Tehran's Polytechnic Institute. For his undergraduate thesis research, Mr. Moghbelli worked under the supervision of Professor Naser Mohammadi in a study "Location tuning of a block copolymer in the interface of PMMA / PBuA latex blends" in the Iranian Polytechnic Institute. Upon graduation, Mr. Moghbelli continued to pursue his graduate research under Professor Sue in Texas A&M University.

Mr. Moghbelli's permanent address is:

3123 Texas A&M University  
Department of Mechanical Engineering  
c/o Dr. Hung-Jue Sue  
College Station, TX, 77843-3123